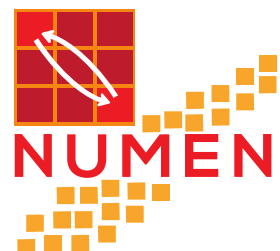




## Terzo Incontro Nazionale di Fisica Nucleare INFN2016

# The NUMEN Project: $^{116}\text{Sn}(\text{O}, \text{Ne})^{116}\text{Cd}$ and $^{116}\text{Cd}(\text{Ne}, \text{O})^{116}\text{Sn}$ DCEX reactions preliminary results

Gianluca Santagati for the NUMEN collaboration

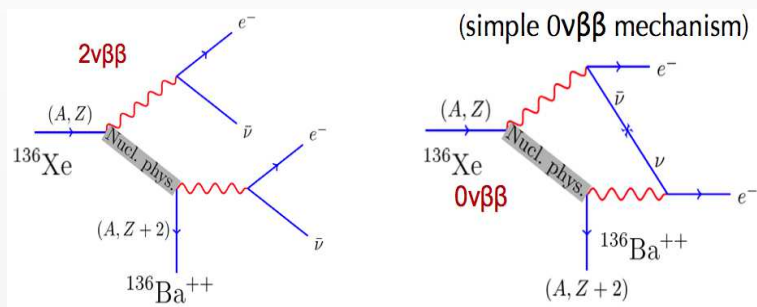


# A basic question in modern Physics



From neutrino oscillations we know  $\rightarrow$  neutrino mass  $\neq 0$

What about the  $m_\nu$  absolute value and the neutrino nature:  
Dirac or Majorana particle?



a) 2v DBD:  $(A, Z) \rightarrow (A, Z+2) + 2e^- + 2\nu_e$

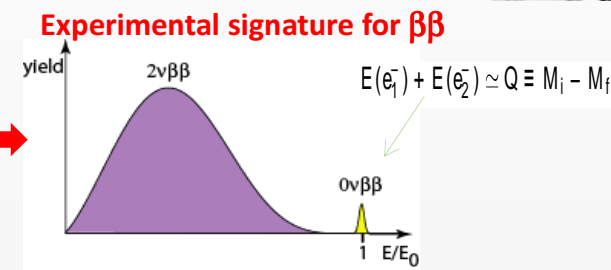
$$T_{1/2} \approx 10^{19-21} \text{ y}$$



Described for the first time  
by Maria Goeppert-Mayer (1935)

b) 0v DBD:  $(A, Z) \rightarrow (A, Z+2) + 2e^-$

$$T_{1/2} > 10^{24} \text{ y}$$



- Respect the conservation law.
- Does not distinguish between Dirac and Majorana
- Experimentally observed in several nuclei

$^{82}\text{Se}, ^{100}\text{Mo}, ^{48}\text{Ca}, ^{76}\text{Ge}, \dots$

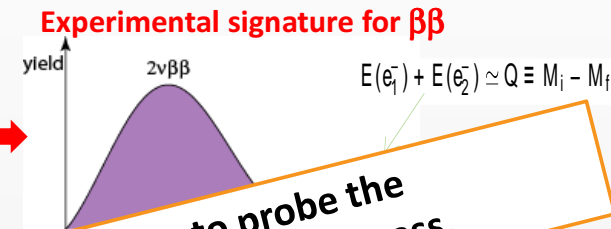
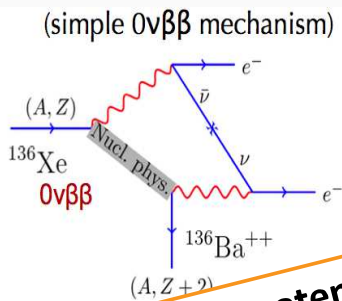
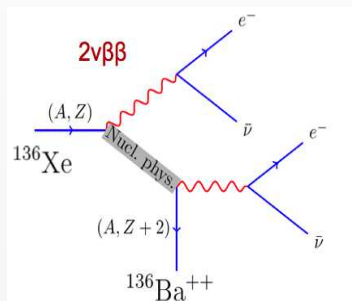
- Neutrino has mass
- Neutrino is Majorana particle
- Violates the leptonic number conservation
- Experimentally not observed
- Forbidden in the Standard Model

# A basic question in modern Physics



From neutrino oscillations we know  $\rightarrow$  neutrino mass  $\neq 0$

What about the  $m_\nu$  absolute value and the neutrino nature:  
Dirac or Majorana particle?



a) 2ν DBD: (A, Z)

The very rare 0νββ decay is potentially the best way to probe the Majorana or Dirac nature of neutrino and to extract its effective mass.

Described for the first time

by Maria Goeppert-Mayer (1935)



b) 0ν DBD: (A, Z)  $\rightarrow$  (A, Z+2) + 2e<sup>-</sup>

$$T_{1/2} > 10^{24} \text{ y}$$

- Does not distinguish between Dirac and Majorana
- Experimentally observed in several nuclei

$^{82}\text{Se}$ ,  $^{100}\text{Mo}$ ,  $^{48}\text{Ca}$ ,  $^{76}\text{Ge}$ , ...

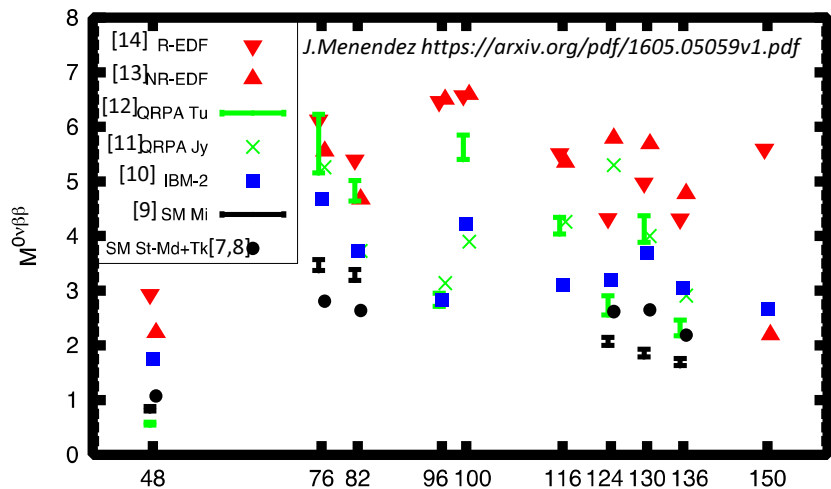
- Neutrino has mass
- Neutrino is Majorana particle
- Violates the leptonic number conservation
- Experimentally not observed
- **Forbidden in the Standard Model**

# The role of nuclear physics

In the  $0\nu\beta\beta$  the decay rate can be expressed as a product of independent factors, that also depends on a function containing physics beyond the Standard Model through the masses and the mixing coefficients of the neutrinos species :

$$1 / T_{1/2}^{0\nu} (0^+ \rightarrow 0^+) = G_{01} \left| M_{\varepsilon}^{0\nu\beta\beta} \right|^2 \left| \frac{\langle m_\nu \rangle}{m_e} \right|^2 \rightarrow \langle m_\nu \rangle = \sum_i |U_{ei}|^2 m_i e^{-i\alpha_i}$$

**new physics inside !**



The differences are about a factor of two to three, or three to four units.

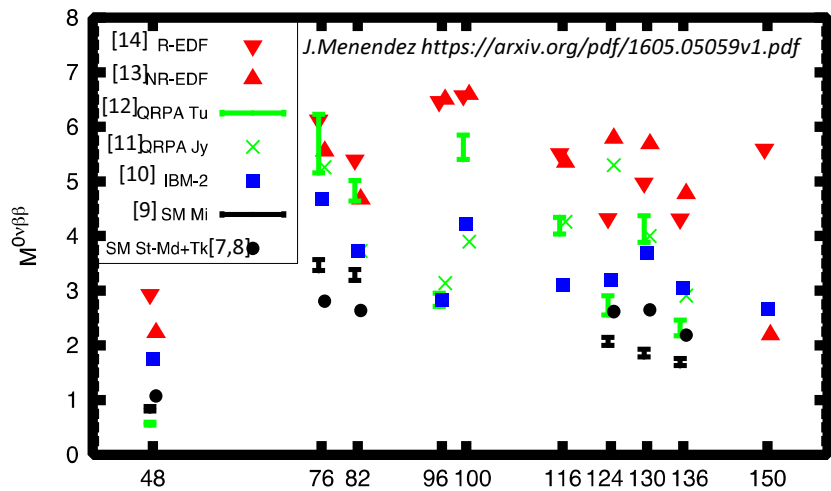
- [7] J. Menéndez, A. Poves, E. Courier and F. Nowacki, Nucl. Phys. A818, 139 (2009)
- [8] Y. Iwata, N. Shimizu, T. Otsuka, Y. Utsuno, J. Menéndez, M. Honma and T. Abe, Phys. Rev. Lett. 116, 112502 (2016).
- [9] A. Neacsu and M. Horoi, Phys. Rev. C93, 024308 (2016).
- [10] J. Barea, J. Kotila and F. Iachello, Phys. Rev. C91, 034304 (2015).
- [11] J. Hyvärinen and J. Suhonen, Phys. Rev. C87, 024613 (2015).
- [12] F. Simkovic, V. Rodin, A. Faessler and P. Vogel, Phys. Rev. C87, 045501 (2013).
- [13] N. López Vaquero, T. R. Rodríguez and J. L. Egido, Phys. Rev. Lett. 111, 142501(2013).
- [14] J. Yao, L. Song, K. Hagino, P. Ring and J. Meng, Phys. Rev.C91, 024316 (2015).

# The role of nuclear physics

In the  $0\nu\beta\beta$  the decay rate can be expressed as a product of independent factors, that also depends on a function containing physics beyond the Standard Model through the masses and the mixing coefficients of the neutrinos species :

$$1 / T_{1/2}^{0\nu} (0^+ \rightarrow 0^+) = G_{01} \left| M_{\varepsilon}^{0\nu\beta\beta} \right|^2 \left| \frac{\langle m_\nu \rangle}{m_e} \right|^2 \rightarrow \langle m_\nu \rangle = \sum_i |U_{ei}|^2 m_i e^{-i\alpha_i}$$

**new physics inside !**



The differences are about a factor of two to three, or three to four units.

Thus, if the  $M^{0\nu\beta\beta}$  nuclear matrix elements were known with sufficient precision, the neutrino mass could be established from  $0\nu\beta\beta$  decay rate measurements.

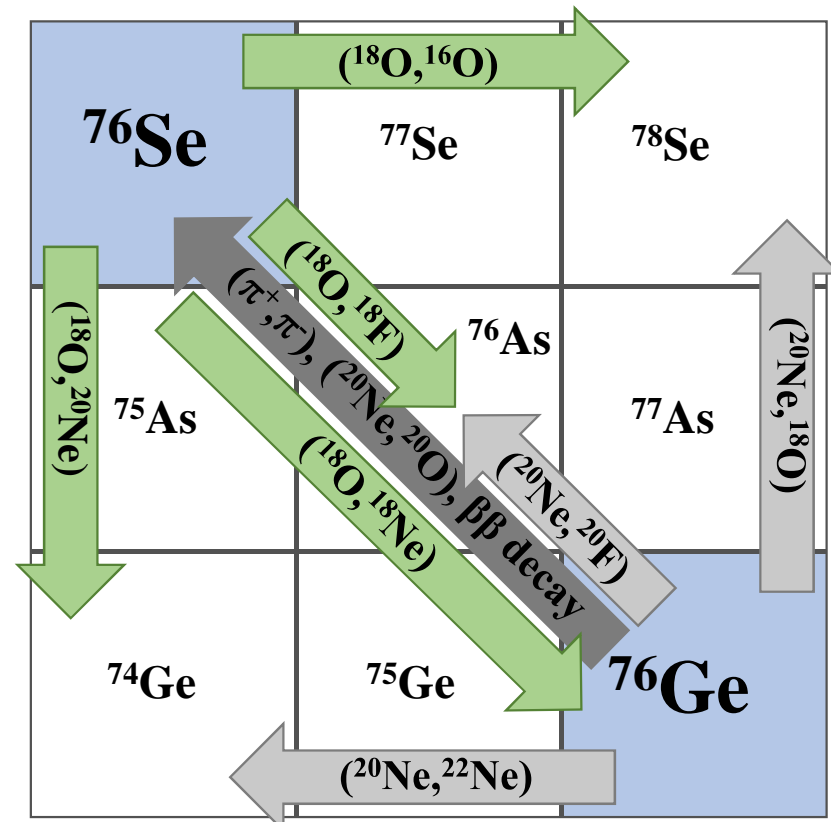
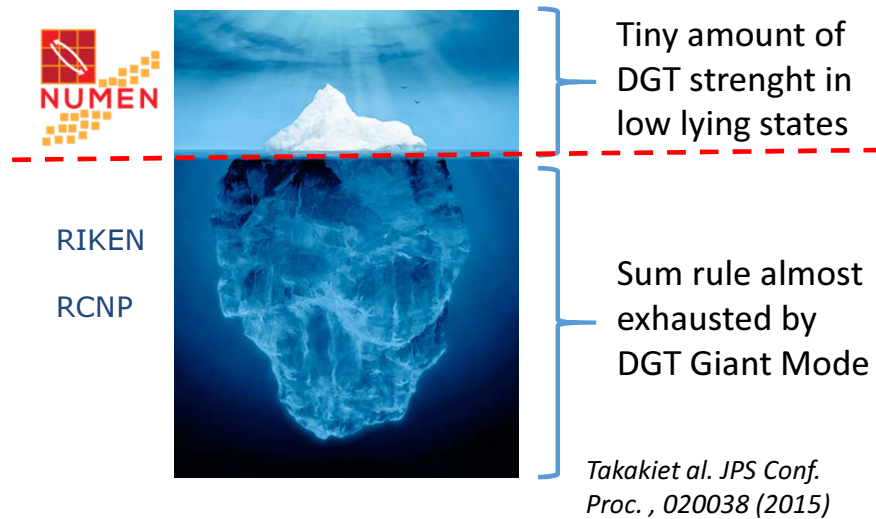
- [7] J. Menéndez, A. Poves, E. Caurier and F. Nowacki, Nucl. Phys. A818, 139 (2009)
- [8] Y. Iwata, N. Shimizu, T. Otsuka, Y. Utsuno, J. Menéndez, M. Honma and T. Abe, Phys. Rev. Lett. 116, 112502 (2016).
- [9] A. Neacsu and M. Horoi, Phys. Rev. C93, 024308 (2016).
- [10] J. Barea, J. Kotila and F. Iachello, Phys. Rev. C91, 034304 (2015).
- [11] J. Hyvärinen and J. Suhonen, Phys. Rev. C87, 024613 (2015).
- [12] F. Simkovic, V. Rodin, A. Faessler and P. Vogel, Phys. Rev. C87, 045501 (2013).
- [13] N. López Vaquero, T. R. Rodríguez and J. L. Egido, Phys. Rev. Lett. 111, 142501(2013).
- [14] J. Yao, L. Song, K. Hagino, P. Ring and J. Meng, Phys. Rev.C91, 024316 (2015).

# Heavy-ion DCE

- ✓ Induced by strong interaction
- ✓ Sequential nucleon transfer mechanism 4<sup>th</sup> order:

Brink's Kinematical matching conditions *D.M.Brink, et al., Phys. Lett. B 40 (1972) 37*

- ✓ Meson exchange mechanism 2<sup>nd</sup> order
- ✓ Possibility to go in both directions



# MAGNEX spectrometer @ LNS

**Camera di scattering**

$$P_i = (x_i, y_i, \theta_i, \phi_i, \delta_i)$$

Quadrupole

Dipole

Good compensation of  
the aberrations:

Trajectory reconstruction

Measured resolutions:

- Energy  $\Delta E/E \sim 1/1000$
- Angle  $\Delta\theta \sim 0.3^\circ$
- Mass  $\Delta m/m \sim 1/160$



Optical characteristics	Values
Maximum magnetic rigidity	1.8 T m
Solid angle	50 msr
Momentum acceptance	-14.3%, +10.3%

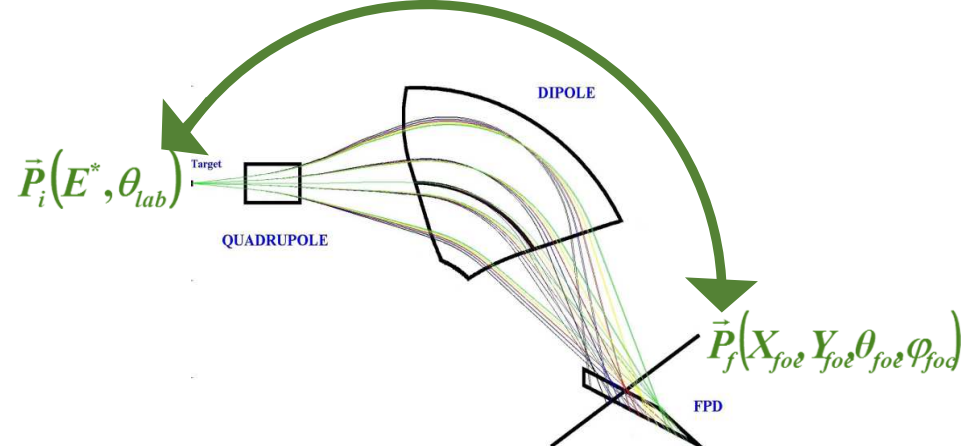
Focal Plane Detector (FPD)

$$P_f = (x_f, y_f, \theta_f, \phi_f)$$

Transport Matrix

$$M: P_i \rightarrow P_f$$

$$M^{-1}: P_f \rightarrow P_i$$



# Factorization of the charge exchange cross-section

**For single CEX:**

$$\frac{d\sigma}{d\Omega}(q, \omega) = \hat{\sigma}_\alpha(E_p, A) F_\alpha(q, \omega) B_T(\alpha) B_P(\alpha) \quad \alpha = \text{Fermi (F) or Gamow-Teller (GT)}$$

**unit cross-section**  $\hat{\sigma}(E_p, A) = K(E_p, 0) |J_\alpha|^2 N_\alpha^D$

T.N.Taddeucci, et al, Nucl. Phys. A 469 (1987) 125

$$B(\alpha) = \frac{1}{2J_i + 1} |M(\alpha)|^2$$

C.J.Guess, et al, PRC 83 064318 (2011)

$\beta$ -decay transition strengths  
(reduced matrix elements)

**B(GT;CEX)/B(GT; $\beta$ -decay)  $\sim 1$**  within a few % especially for the strongest transitions

In the hypothesis of a surface localized process (for direct quasi elastic processes), in a simple model one can assume that the DCE process is just a second order charge exchange, where projectile and target exchange two uncorrelated isovector virtual mesons.

**Generalization to DCE:**

In analogy to the single charge-exchange, the dependence of the cross-section from  $q$  is represented by a Bessel function.

$$\frac{d\sigma^{DCE}}{d\Omega}(q, \omega) = \hat{\sigma}_\alpha^{DCE}(E_p, A) F_\alpha^{DCE}(q, \omega) B_T^{DCE}(\alpha) B_P^{DCE}(\alpha)$$

**unit cross-section**  $\hat{\sigma}_\alpha^{DCE}(E_p, A) = K(E_p, 0) |J_\alpha^{DCE}|^2 N_\alpha^D$

# The NUMEN goals

1. **The aim of the NUMEN Project** : Towards the access of the NME involved in the half-life of the  $0\nu\beta\beta$  decay by measuring the cross sections of **HI induced DCE reactions** with high accuracy.

$$1/T_{1/2}^{0\nu} (0^+ \rightarrow 0^+) = G_0 |M^{\beta\beta\,0\nu}|^2 \left| \frac{\langle m_\nu \rangle}{m_e} \right|^2$$

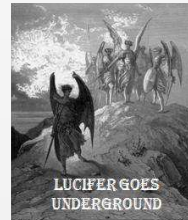
2. A new generation of **DCE constrained  $0\nu\beta\beta$  NME theoretical calculations can emerge**: the measured DCE cross sections provide a powerful tool for theory in order to give very stringent constraints in the NME estimation. The DCE processes can be artificially generated in the lab.
3. The ratio of measured cross sections **can give a model independent way to compare the sensitivity of different half-life experiments**.



$^{76}\text{Ge}$



$^{130}\text{Te}$



$^{82}\text{Se}$



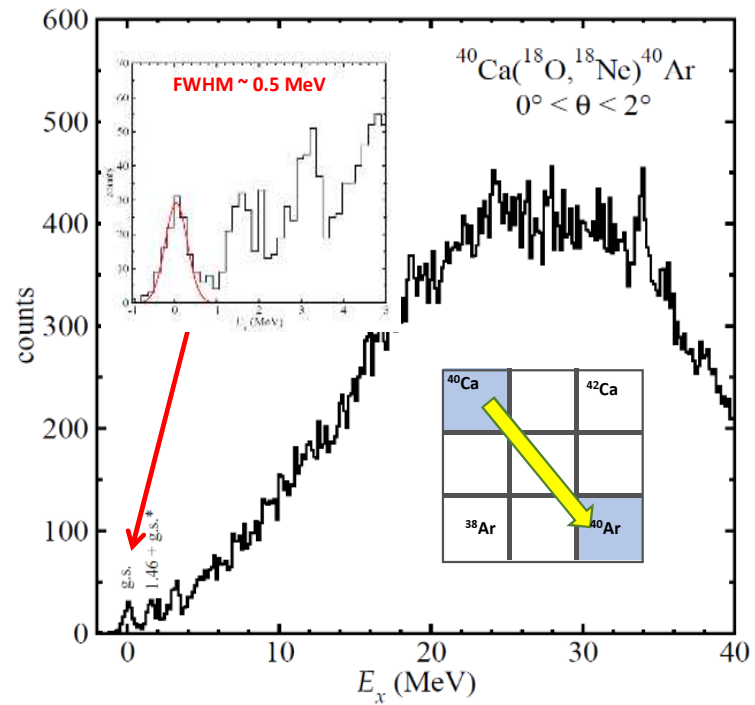
$^{136}\text{Xe}$



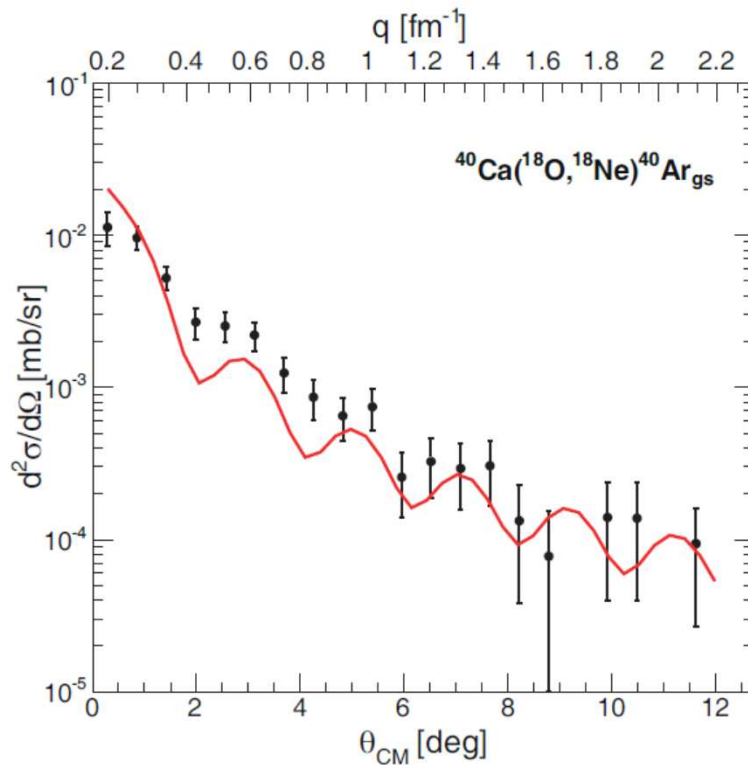
$^{116}\text{Cd}$

**Strong impact in future development of the field,  
looking for a “golden isotope” ...**

# The pilot experiment: $^{40}\text{Ca}(^{18}\text{O}, ^{18}\text{Ne})^{40}\text{Ar}$ @ LNS



Measured energy spectrum of  $^{40}\text{Ar}$  at very **forward angles** with an energy resolution of **FWHM  $\sim 0.5$  MeV**.



The position of the minima is well described by a Bessel function: such an oscillation pattern is not expected in complex multistep transfer reactions.

F. Cappuzzello, et al., Eur. Phys. J. A (2015) 51: 145

$$\sigma^{\text{DCE}} = 260 \text{ nb} \quad 0^\circ < \theta < 2^\circ$$

## NUMEN experimental runs

**March 2016**  $^{116}\text{Cd} + ^{20}\text{Ne}$  @ 15-22 MeV/u (test) at  $\vartheta_{\text{opt}} = -3^\circ$  ( $0^\circ < \theta_{\text{lab}} < 8^\circ$ )

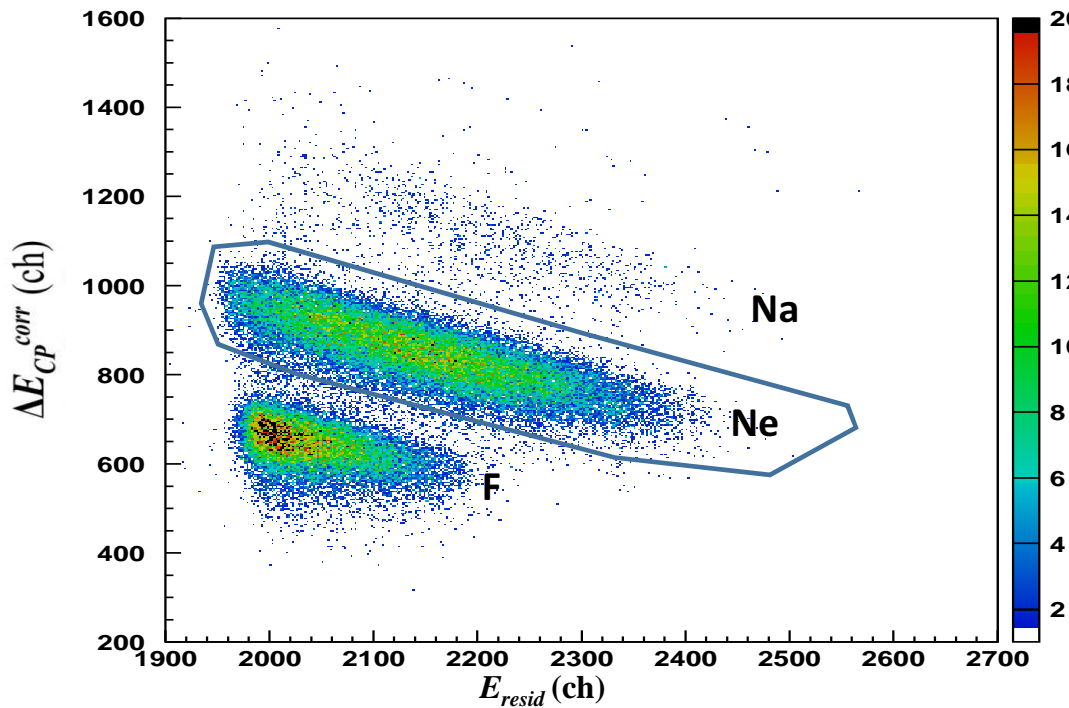
- DCEX reaction  $^{116}\text{Cd}(^{20}\text{Ne}, ^{20}\text{O})^{116}\text{Sn}$
- CEX reaction  $^{116}\text{Cd}(^{20}\text{Ne}, ^{20}\text{F})^{116}\text{In}$
- 2p-transfer  $^{116}\text{Cd}(^{20}\text{Ne}, ^{18}\text{O})^{118}\text{Sn}$
- 1p-transfer  $^{116}\text{Cd}(^{20}\text{Ne}, ^{19}\text{F})^{117}\text{In}$

**October 2015 - June 2016**  $^{116}\text{Sn} + ^{18}\text{O}$  @ 15 MeV/u at  $\vartheta_{\text{opt}} = 3^\circ$  ( $0^\circ < \theta_{\text{lab}} < 9^\circ$ )

- DCEX reaction  $^{116}\text{Sn}(^{18}\text{O}, ^{18}\text{Ne})^{116}\text{Cd}$
- CEX reaction  $^{116}\text{Sn}(^{18}\text{O}, ^{18}\text{F})^{116}\text{In}$
- 2p-transfer  $^{116}\text{Sn}(^{18}\text{O}, ^{20}\text{Ne})^{114}\text{Cd}$
- 1p-transfer  $^{116}\text{Sn}(^{18}\text{O}, ^{19}\text{F})^{115}\text{In}$
- 2n-transfer  $^{116}\text{Sn}(^{18}\text{O}, ^{16}\text{O})^{118}\text{Sn}$

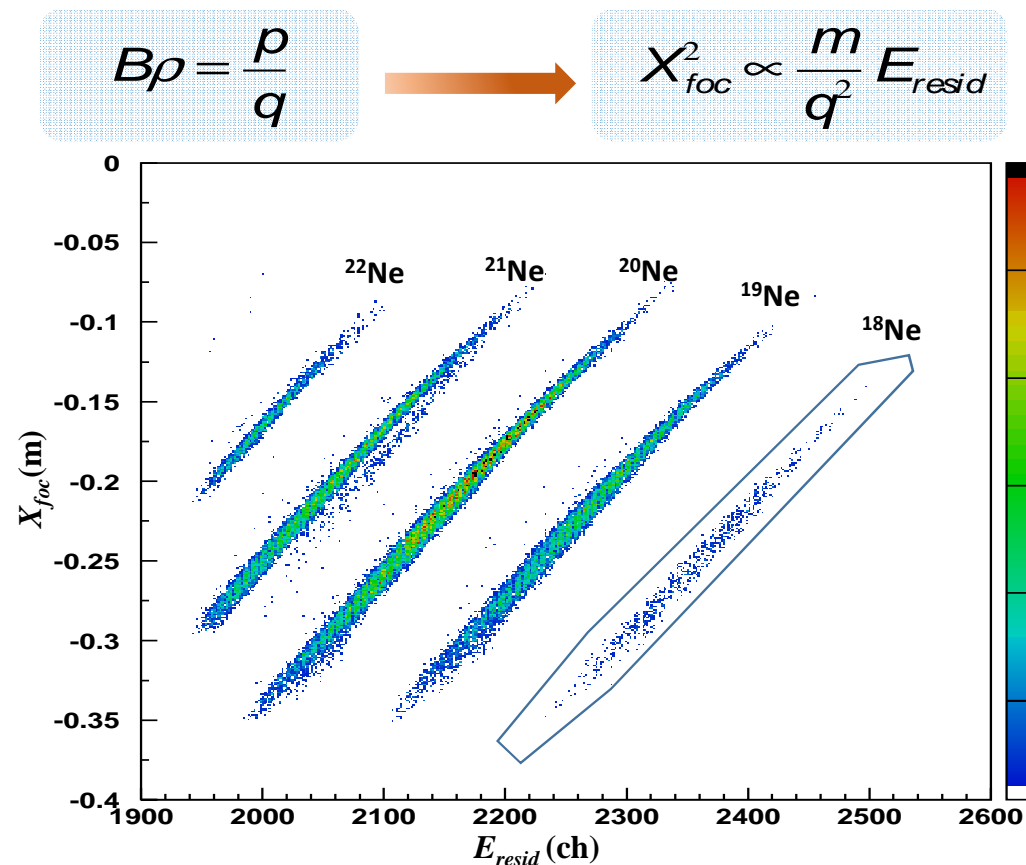
# $^{116}\text{Sn}(\text{O},\text{Ne})^{116}\text{Cd}$ DCEX data reduction

Z identification

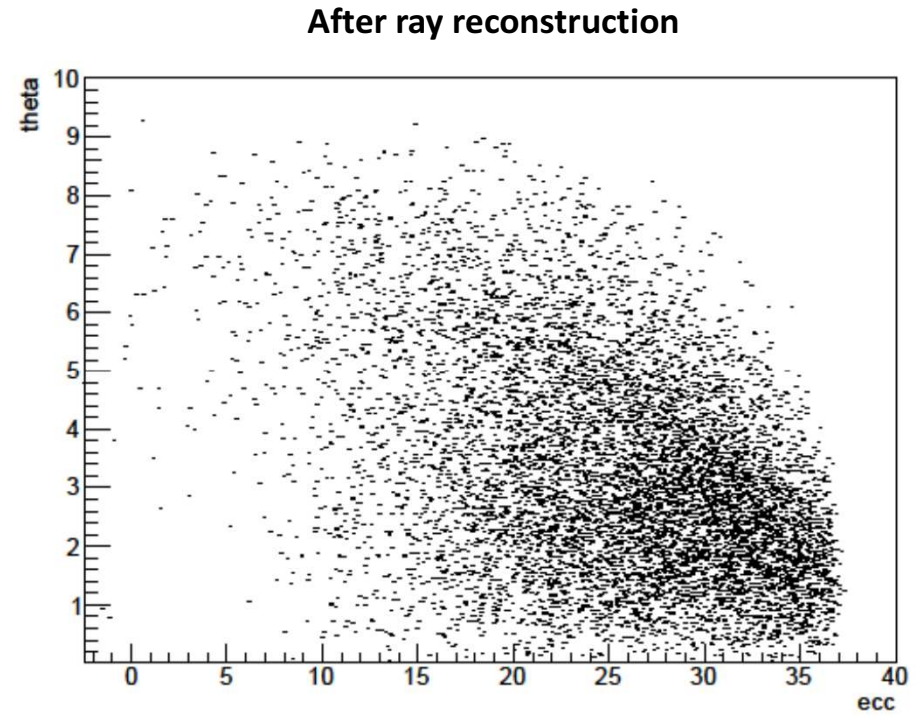
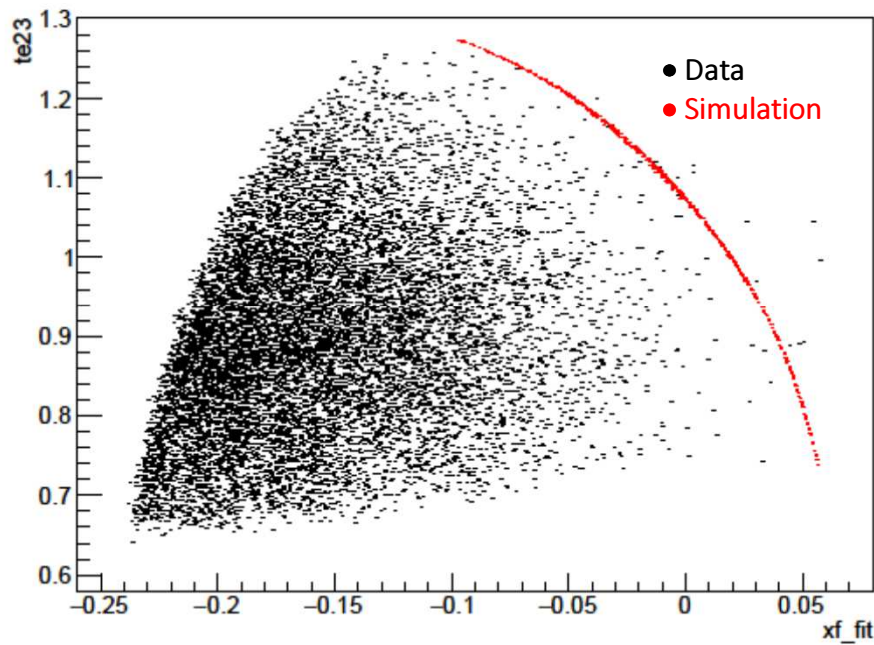


- A. Cunsolo, et al., NIMA484 (2002) 56
- A. Cunsolo, et al., NIMA481 (2002) 48
- F. Cappuzzello et al., NIMA621 (2010) 419
- F. Cappuzzello, et al. NIMA638 (2011) 74

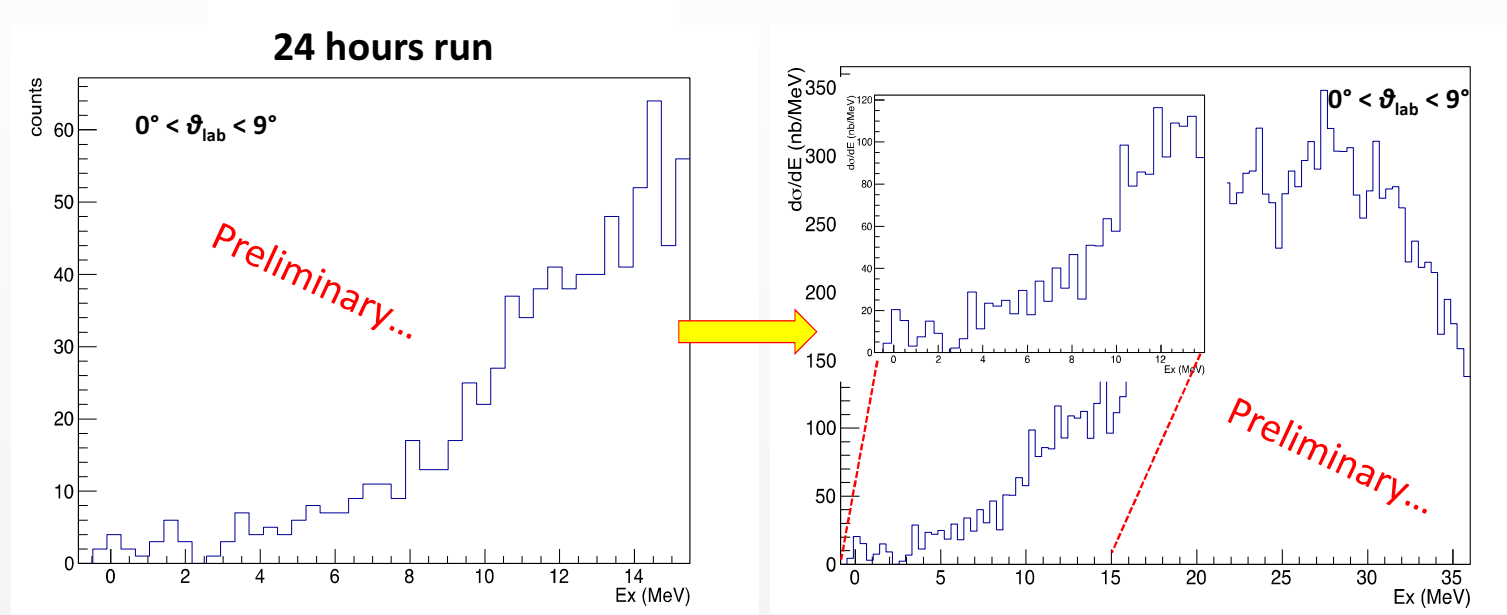
A identification



# $^{116}\text{Cd}(^{20}\text{Ne}, ^{20}\text{O})^{116}\text{Sn}$ DCEX reaction @ 15 MeV/A



# $^{116}\text{Cd}(^{20}\text{Ne}, ^{20}\text{O})^{116}\text{Sn}$ DCEX reaction @ 15 MeV/A

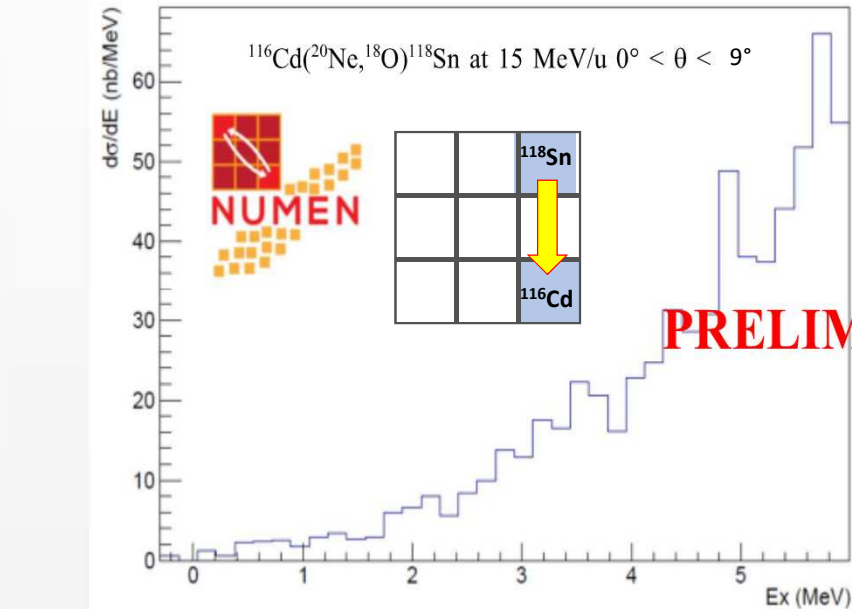


DCE transitions to  $^{116}\text{Sn}_{\text{gs}}$  and first excited  $2^+$  state at 1.29 MeV are clearly separated (energy resolution  $\sim 0.75$  MeV) and characterized by a remarkable cross section of about 66 nb and 38 nb, respectively.

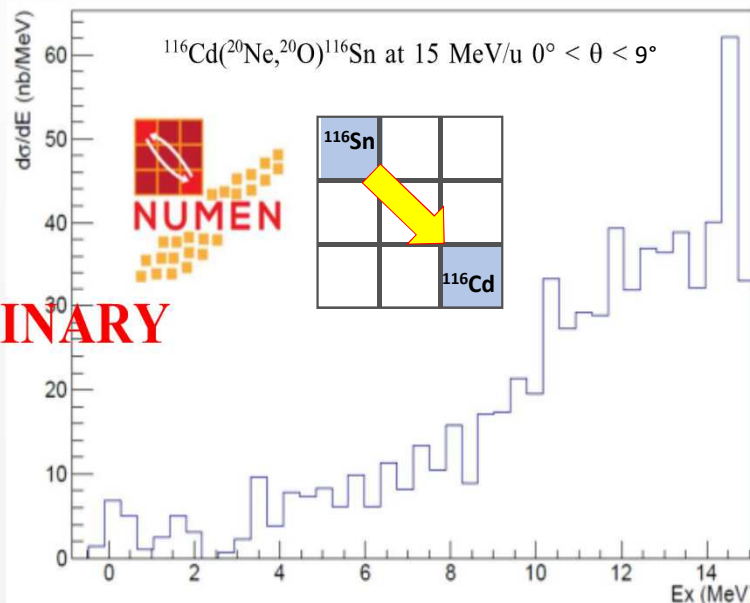


# The role of the competing processes

Multi nucleon transfer suppressed respect to DCE



Energy spectrum ( $\text{Ex} = Q_0 - Q$ ) of the  $^{116}\text{Cd}(^{20}\text{Ne}, ^{18}\text{O})^{118}\text{Sn}$  two-proton stripping reaction at 15 MeV/u  $0^\circ < \vartheta_{\text{lab}} < 9^\circ$



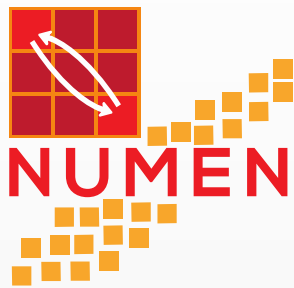
Reconstructed energy spectrum of the  $^{116}\text{Cd}(^{20}\text{Ne}, ^{20}\text{O})^{116}\text{Sn}$  DCE reaction at 15 MeV/u  $0^\circ < \vartheta_{\text{lab}} < 9^\circ$



1. Theoretical upgrade → New Structure and Dynamic calculations
2. Present technology is not enough to measure at very high rates of heavy ions! → Cs and Magnex upgrade

## Magnex upgrade:

- FPD gas tracker → GEM - like tracker system
  - Si detectors → SiC detectors
  - new Front-End electronics
- 
- array of detectors for measuring the coincident  $\gamma$ -rays
  - enhancement of the maximum magnetic rigidity



# NUMEN

NUclear Matrix Elements for Neutrinoless  
double beta decay





C. Agodi, J. Bellone, R. Bijker, D. Bonanno, D. Bongiovanni, V. Branchina, M.P. Bussa, L. Busso, L. Calabretta, A. Calanna, D. Calvo, F. Cappuzzello, D. Carbone, M. Cavallaro, M. Colonna, G. D'Agostino, N. Deshmukh, S. Ferrero, A. Foti, P. Finocchiaro, G. Giraudo, V. Greco, F. Iazzi, R. Introzzi, G. Lanzalone, A. Lavagno, F. La Via, J.A. Lay, G. Litrico, D. Lo Presti, F. Longhitano, A. Muoio, L. Pandola, F. Pinna, S. Reito, D. Rifuggiato, M.V. Ruslan, G. Santagati, E. Santopinto, L. Scaltrito, S. Tudisco

INFN - Laboratori Nazionali del Sud, Catania, Italy, INFN - Sezione di Catania, Catania, Italy Dipartimento di Fisica e Astronomia, Università di Catania, Catania, Italy, INFN - Sezione di Torino, Torino, Italy, Politecnico di Torino, Italy INFN - Sezione di Genova, Genova, Italy, CNR-IMM, Sezione di Catania, Italy, Università degli Studi di Enna "Kore", Enna, Italy

T. Borello-Lewin, P. N. de Faria, J.L. Ferreira, R. Linares, J. Lubian, N.H. Medina, J.R.B. Oliveira, M.R.D. Rodrigues, D.R. Mendes Junior, V. Zagatto

Instituto de Física, Universidade Federal Fluminense, Niterói, RJ, Brazil

Instituto de Física, Universidade de São Paulo, São Paulo, SP, Brazil

X. Aslanoglou, A. Pakou, O. Sgouros, V. Soukeras, G. Souliotis,

Department of Physics and HINP, The University of Ioannina, Ioannina, Greece

Department of Chemistry and HINP, National and Kapodistrian University of Athens, Greece

E. Aciksoz, I. Boztosun, A. Hacisalihoglu, S.O. Solakci,

Akdeniz University, Antalya, Turkey

L. Acosta, E.R. Chávez Lomelí,

Universidad Nacional Autónoma de México

S. Boudhaim, M.L. Bouhssa, Z. Housni, A. Khouaja, J. Inchaou

Université Hassan II – Casablanca, Morocco

N. Auerbach,

School of Physics and Astronomy Tel Aviv University, Israel

H. Lenske,

University of Giessen, Germany

# Thank you !



NUMEN 2015 Workshop - LNS 1-2 dicembre 2015



Spokespersons: C. Agodi ([agodi@lns.infn.it](mailto:agodi@lns.infn.it)), F. Cappuzzello ([cappuzzello@lns.infn.it](mailto:cappuzzello@lns.infn.it)) \

Back-up slides

# $0\nu\beta\beta$ vs HI-DCE

1. **Initial and final states**: Parent/daughter states of the  $0\nu\beta\beta$  are the same as those of the target/residual nuclei in the DCE;
2. **Spin-Isospin mathematical structure** of the transition operator: Fermi, Gamow-Teller and rank-2 tensor together with higher L components are present in both cases;
3. **Large momentum available**: A linear momentum as high as 100 MeV/c or so is characteristic of both processes;
4. **Non-locality**: both processes are characterized by two vertices localized in two valence nucleons. In the ground to ground state transitions in particular a pair of protons/neutrons is converted in a pair of neutrons/protons so the non-locality is affected by basic pairing correlation length;
5. **In-medium** processes: both processes happen in the same nuclear medium, thus quenching phenomena are expected to be similar;
6. **Relevant off-shell propagation** in the intermediate channel: both processes proceed via the same intermediate nuclei off-energy-shell even up to 100 MeV.

# Planned experimental activity

NUclear REactions for neutrinoless double beta decay

Reactions	2017	2018	2019
$^{20}\text{Ne} + ^{116}\text{Cd}$ at 15 MeV/u	~ 60 BTU		
$^{18}\text{O} + ^{40}\text{Ca}$ at 25 MeV/u		~ 45 BTU	
$^{18}\text{O} + ^{76}\text{Se}$ at 15 MeV/u		~ 75 BTU	
$^{20}\text{Ne} + ^{76}\text{Ge}$ at 15 MeV/u		~ 60 BTU	
$^{20}\text{Ne} + ^{116}\text{Cd}$ at 25 MeV/u			~ 60 BTU
$^{20}\text{Ne} + ^{76}\text{Ge}$ at 25 MeV/u			~ 60 BTU

# From the pilot experiment towards the “hot cases”: The four phases of NUMEN project

## ➤ **Phase1: the experiment feasibility**

$^{40}\text{Ca}(\text{O}^{18},\text{Ne}^{18})\text{Ar}$  @ 270 MeV already done: the results demonstrate the technique feasibility.

## ➤ **Phase2: toward “few hot” cases optimizing experimental conditions and getting first result**

Upgrading of CS and MAGNEX, preserving the access to the present facility. Tests will be crucial.

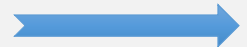
## ➤ **Phase3: the facility upgrade**

Disassembling of the old set-up and re-assembling of the new ones will start: about 18-24 months

## ➤ **Phase4: the experimental campaign**

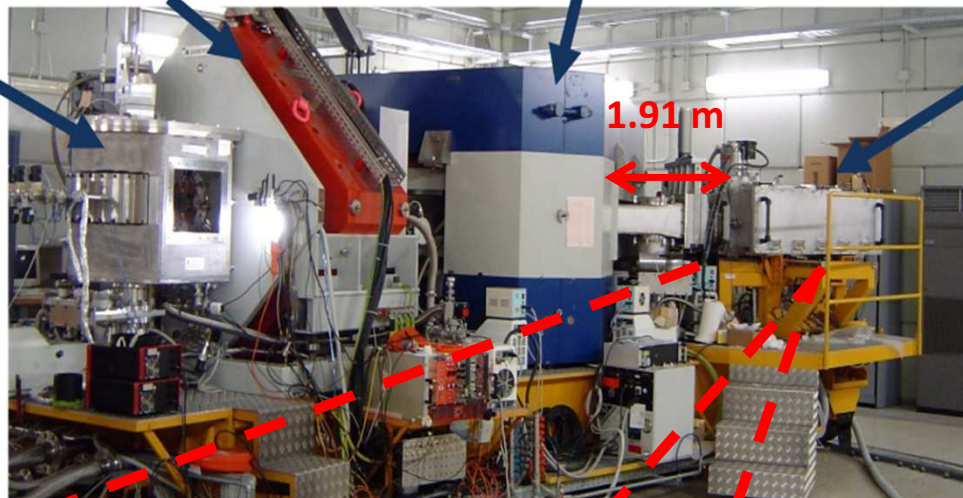
High beam intensities (some pA) and long experimental runs to reach integrated charge of hundreds of mC up to C, for the experiments in coincidences, for all the variety of isotopes for  $0\nu\beta\beta$  decay ( $^{48}\text{Ca}$ ,  $^{82}\text{Se}$ ,  $^{96}\text{Zr}$ ,  $^{100}\text{Mo}$ ,  $^{110}\text{Pd}$ ,  $^{124}\text{Sn}$ ,  $^{128}\text{Te}$ ,  $^{136}\text{Xe}$ ,  $^{148}\text{Nd}$ ,  $^{150}\text{Nd}$ ,  $^{154}\text{Sm}$ ,  $^{160}\text{Gd}$ ,  $^{198}\text{Pt}$ ).

year	PRELIMINARY TIME TABLE								
	2013	2014	2015	2016	2017	2018	2019	2020	
Phase1									
Phase2									
Phase3									
Phase4									





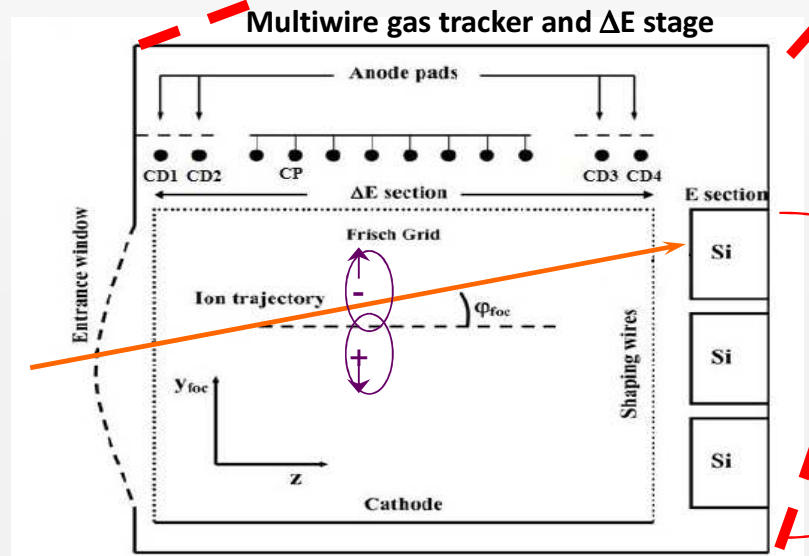
Quadrupole  
Scattering Chamber



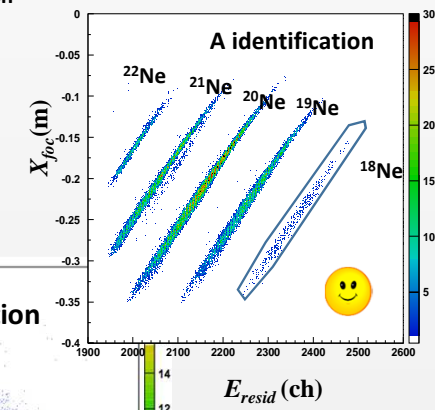
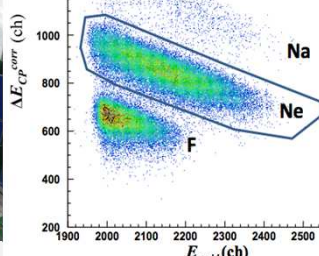
Focal Plane  
Detector  
active area  
**140x20 cm<sup>2</sup>**

a ionization drift chamber, five independent proportional counters, four of which are position-sensitive and a wall of stopping silicon detectors.

Pure isobutane pressure range: 5-100mbar; 600-800 Volt, wires 20 micron



Wall of 60 stopping 7 X 5 cm<sup>2</sup> Silicon detectors surface covered 100 X 21 cm<sup>2</sup>



$$B\rho = \frac{p}{q}$$

$$X_{foc}^2 \propto \frac{m}{q^2} E_{resid}$$

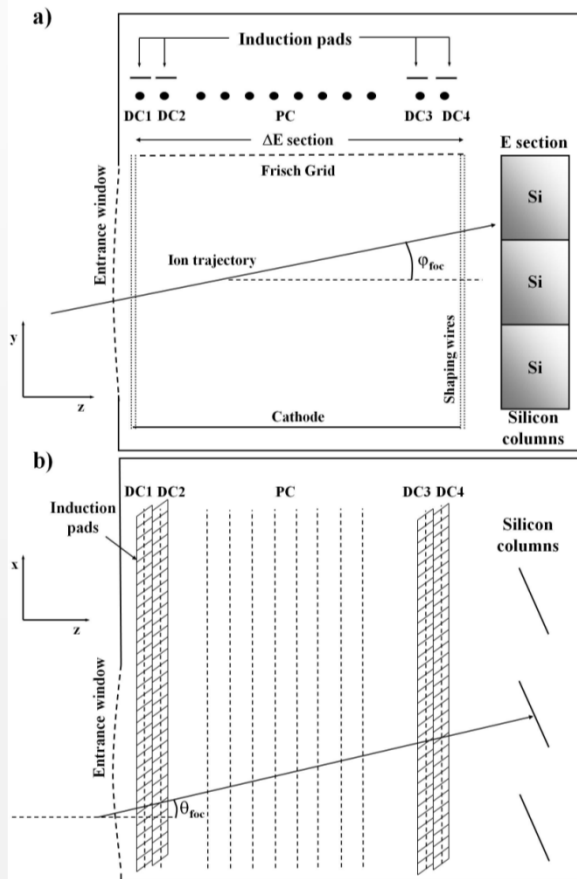
# MAGNEX Focal Plane Detector

- Gas-filled hybrid detector

Drift chamber 1400mm x200mmx100mm

Pure isobutane pressure range: 5-100 mbar; 600-800 V,wires 20 micron

Schematic view of the MAGNEX Focal Plane Detector: a) side view; b) top view.



60 Silicon Detectors

→  $E_{res}$

**Ion identification**

5 Proportional Wires

→  $\Delta E$

4 Induction Strip

→  $X_1, X_2, X_3, X_4$

→  $X_{foc}, \theta_{foc}$

4 Drift Chamber (DC)

→  $Y_1, Y_2, Y_3, Y_4$

→  $Y_{foc}, \phi_{foc}$

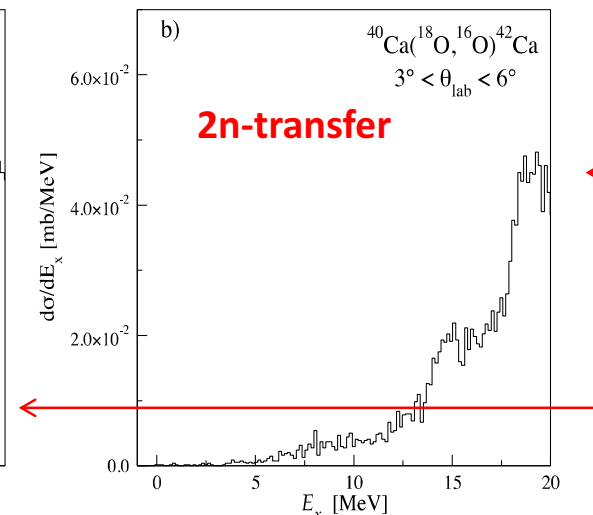
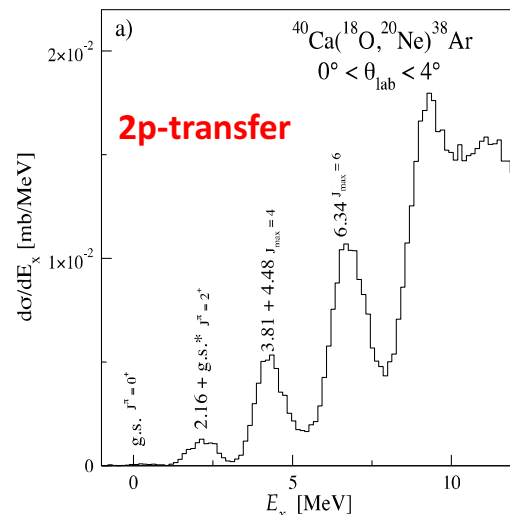
**Ray-reconstruction**



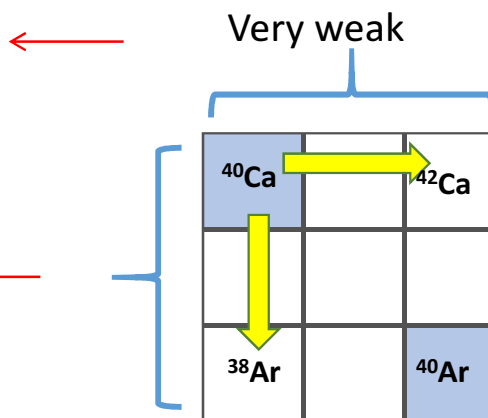
- Wall Si 500  $\mu$ m  
20 columns, 3 rows



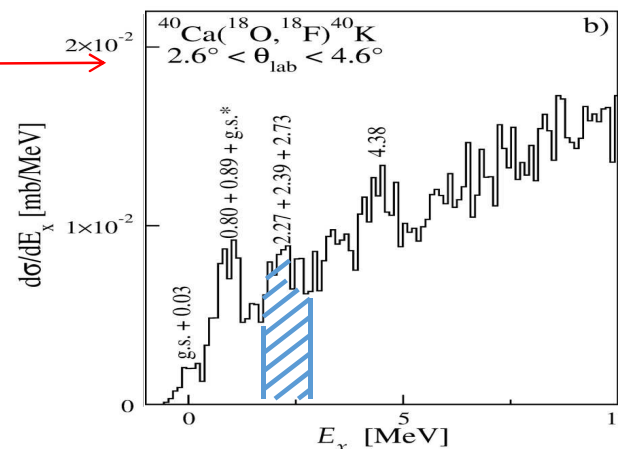
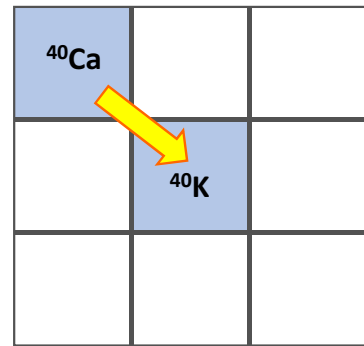
# The role of the transfer reaction and the competing processes



Less than 1% effect in  
the DCE cross section



single charge exchange



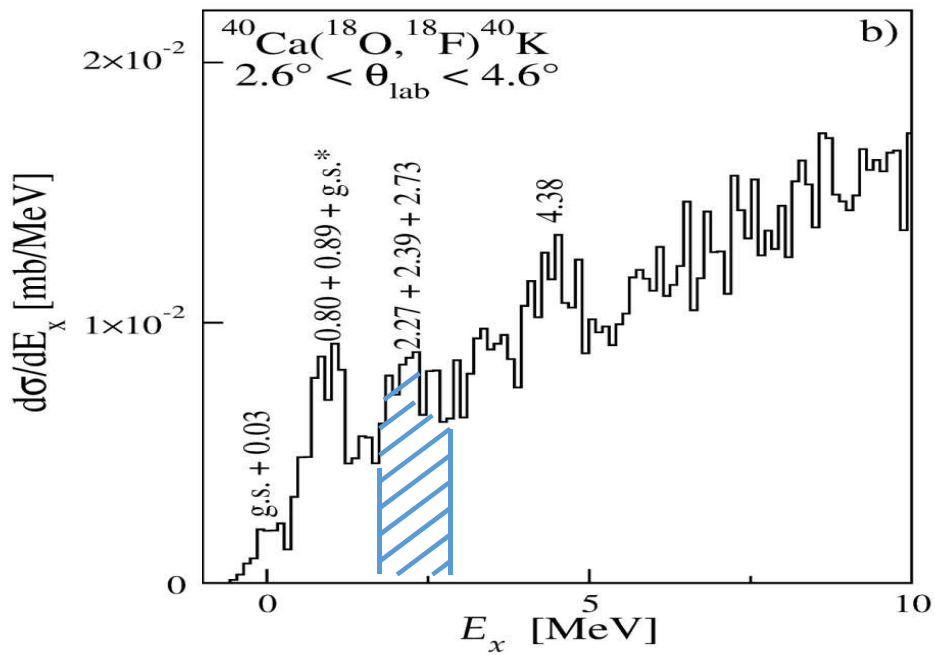
x-section ( $2\text{MeV} < E_x < 3\text{MeV}$ )  
 $\approx 0.5 \text{ mb/sr}$

Extracted  $B(\text{GT}) = 0.087$

$B(\text{GT})$  from  $(^3\text{He}, t)$  = 0.083  
Y. Fujita

# HI Single CEX @ LNS

$^{40}\text{Ca}(\text{O}, \text{F})^{40}\text{K}$  @ 15 MeV/u

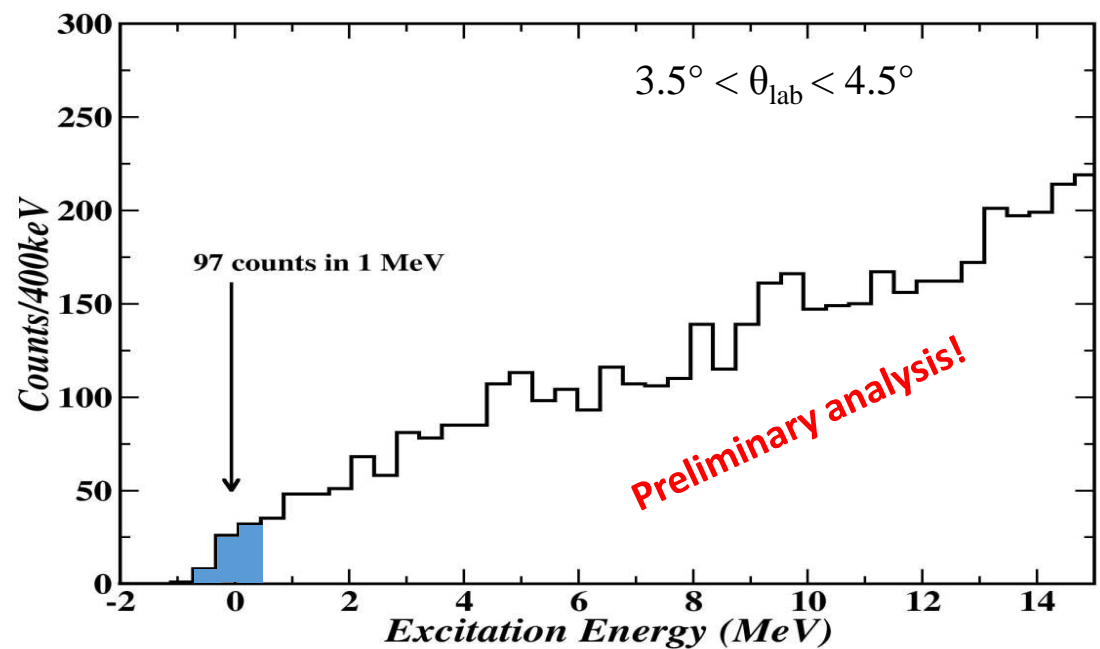


x-section ( $2\text{MeV} < E_x < 3\text{MeV}$ )  
 $\approx 0.5 \text{ mb/sr}$

Extracted B(GT) = 0.087

B(GT) from ( $^3\text{He}, t$ ) = 0.083  
 Y. Fujita

$^{116}\text{Sn}(\text{O}, \text{F})^{116}\text{In}$  @ 25 MeV/u



x-section (within 1 MeV)  
 $\approx 0.17 \text{ mb/sr}$

Extracted upper limit for B(GT) < 0.8

B(GT) from ( $d, ^2\text{He}$ ) = 0.4  
 S.Rakers, et al., PRC 71 (2005) 054313

## The pilot experiment: $^{40}\text{Ca}(^{18}\text{O}, ^{18}\text{Ne})^{40}\text{Ar}$ @LNS

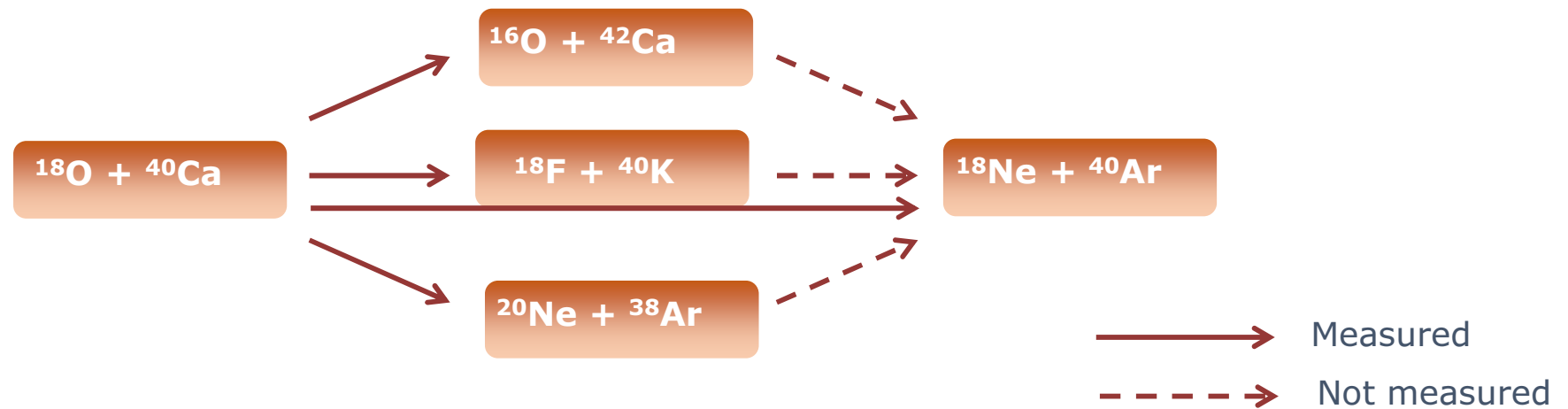
➤  $^{18}\text{O}^{7+}$  beam from LNS Cyclotron at 270 MeV (10 pnA)

➤  $^{40}\text{Ca}$  solid target of 300  $\mu\text{g}/\text{cm}^2$

➤ Ejectiles detected by the MAGNEX spectrometer

➤ Angular setting

$$\theta_{opt} = 4^\circ \longrightarrow -2^\circ < \theta_{lab} < 10^\circ$$



### *Analogia con il decadimento $\beta$*

L'interazione forte nucleone-nucleone  $V_{NN}$  presenta

$$V_{NN} \equiv V_{ij}(r_{ij}) = V_O + V_\sigma(\vec{\sigma}_i \cdot \vec{\sigma}_j) + V_{SO}(\vec{S} \cdot \vec{L}) + V_T S_T + \tau_i \cdot \tau_j [V_\tau + V_{\sigma\tau}(\vec{\sigma}_i \cdot \vec{\sigma}_j) + V_{SO}^\tau(\vec{S} \cdot \vec{L}) + V_T^\tau S_T]$$

*Fermi-like      Gamow Teller-like*

→ ampiezze di transizioni hanno struttura molto simile a quelle del decadimento  $\beta$  essendo tali transizioni permesse ( $L=0$ ) distinte in:

- Fermi,  $S=0 \rightarrow \Delta J=0$  e  $O_F=\tau^\pm$
  - Gamow-Teller,  $S=1 \rightarrow \Delta J=1$  e  $O_{GT}=\sigma\tau^\pm$

Connessione tra decadimento  $\beta$  e reazioni di scambio di carica notata alla fine degli anni '50<sup>1)</sup>.

Formalizzata<sup>3)</sup> per sistemi leggeri, sotto opportune condizioni ( $q \sim 0$ ,  $L=0$ ) vale la fattorizzazione:

$$\frac{d\sigma}{d\Omega}(q, E_x) = \hat{\sigma}_\alpha(E_p, A) F_\alpha(q, E_x) B_T(\alpha) B_p(\alpha)$$

Espressione che vale anche per ioni pesanti entro un 20-30% di precisione

<sup>1)</sup> Bloom et al, Phys. Rev. Lett. 3 (1959).

<sup>2)</sup> C.D. Goodman et al, Phys. Rev. Lett. 44 (1980).

<sup>3)</sup> T. Taddeucci et al, Phys. Rev. C 28 (1983).

# The volume integrals

## Nuclear spin and isospin excitations

Franz Osterfeld

Reviews of Modern Physics, Vol. 64, No. 2, April 1992

- ✓ Volume integrals are **larger at smaller energies**
- ✓ They enter to the **fourth power** in the unit cross section!
- ✓ **GT-F competition** at low energy

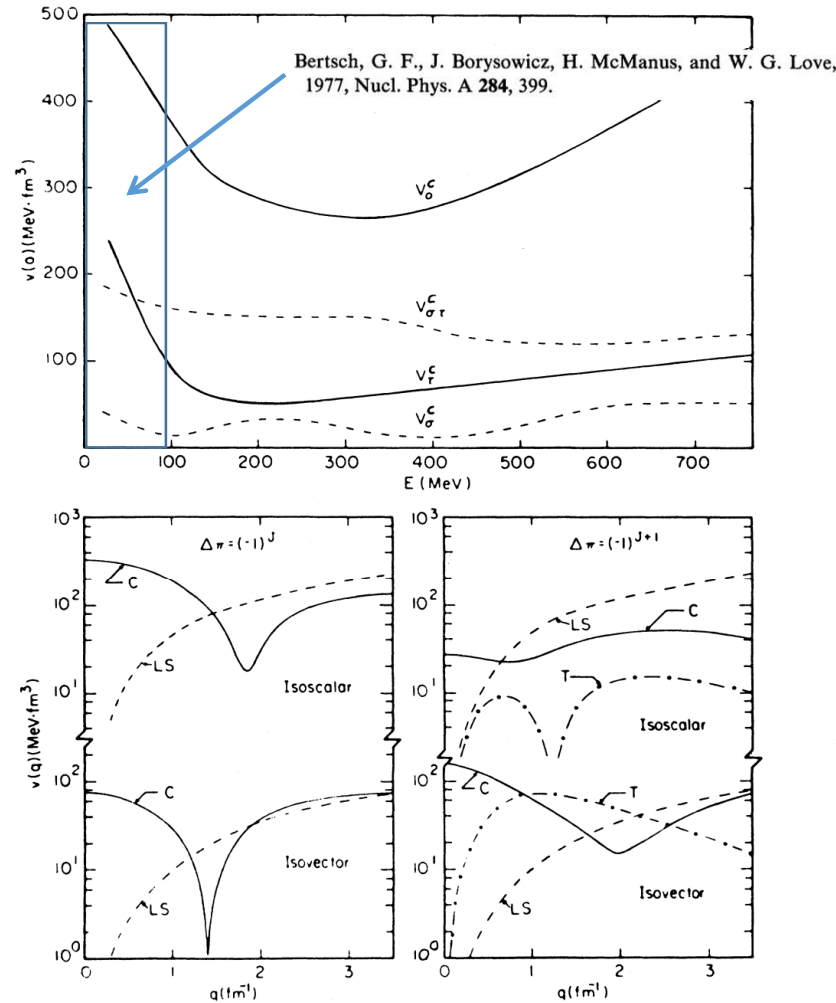
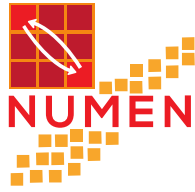


FIG. 15. Energy and momentum dependence of the free nucleon-nucleon  $t_F$  matrix. The upper part of the figure shows the energy dependence of the central components of the effective  $t_F$  matrix at zero-momentum transfer (including direct and exchange terms). The  $G$ -matrix interaction of Bertsch *et al.* (1977) was used below 100 MeV and joined smoothly to the  $t_F$  matrix above 100 MeV. The lower figures show the momentum dependence of the 135-MeV  $t_F$  matrix for natural-(left figure) and unnatural-(right figure) parity transitions. Isoscalar and isovector central ( $C$ ), spin-orbit ( $LS$ ), and tensor ( $T$ ) components are shown. From Petrovich and Love (1981).



# Factorization of the double charge exchange cross-section



Under the hypothesis of surface localization, one can assume that the DCE process is just a second order charge exchange: **DCE cross sections can be factorized** in a **nuclear structure term, containing the matrix element**, and a **nuclear reaction factor**.

## generalization to DCE:

In analogy to the single charge-exchange, the dependence of the cross-section from  $q$  is represented by a Bessel function.

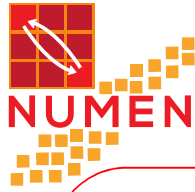
$$\frac{d\sigma^{DCE}}{d\Omega}(q, \omega) = \hat{\sigma}_\alpha^{DCE}(E_p, A) F_\alpha^{DCE}(q, \omega) B_T^{DCE}(\alpha) B_P^{DCE}(\alpha)$$

## unit cross-section

$$\hat{\sigma}_\alpha^{DCE}(E_p, A) = K(E_p, 0) |J_\alpha^{DCE}|^2 N_\alpha^D$$

A wide range of DCE cross sections has never been accurately measured due to :

- The difficult to perform **zero degrees** measurements.
- The poor yields in the measured energy spectra and angular distributions, **due to the very low cross sections**.
- The difficulty to disentangle possible contributions of **multi-nucleon transfer reactions** leading to the same final state.



# Factorization of the charge exchange cross-section



*for single CEX:*

$\alpha$  = Fermi (F)  
or Gamow Teller (GT)

**unit cross-section**

$$\frac{d\sigma}{d\Omega}(q, \omega) = \hat{\sigma}_\alpha(E_p, A) F_\alpha(q, \omega) B_T(\alpha) B_P(\alpha)$$

$$B(\alpha) = \frac{1}{2J_i + 1} |M(\alpha)|^2$$

$\beta$ -decay transition strengths  
(reduced matrix elements)

C.J. Guess, et al, PRC 83 064318 (2011)

T.N. Taddeucci, et al, Nucl. Phys. A 469 (1987) 125

The factor  $F_\alpha(q, \omega)$  describes the shape of the cross-section distribution as a function of the linear momentum transfer and the excitation energy.

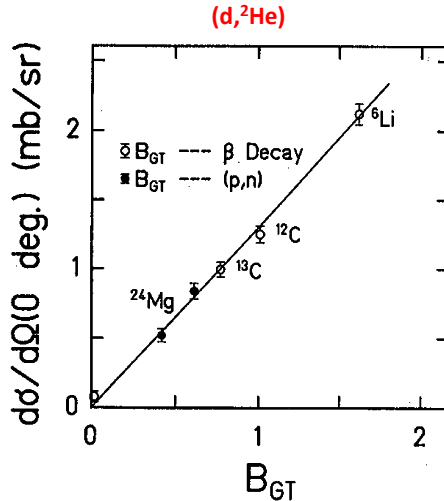


Fig. 12. The measured cross-sections of the  $(d, {}^2\text{He})$  reactions at 03 as a function of the  $G^+$  strengths deduced from  $\beta$ -decay or  $(p, n)$  reaction studies. The solid line is a linear "t" to the data [24].

$B(\text{GT}; \text{CEX})/B(\text{GT}; \beta\text{-decay}) \sim 1$  within a few % especially for the strongest transitions

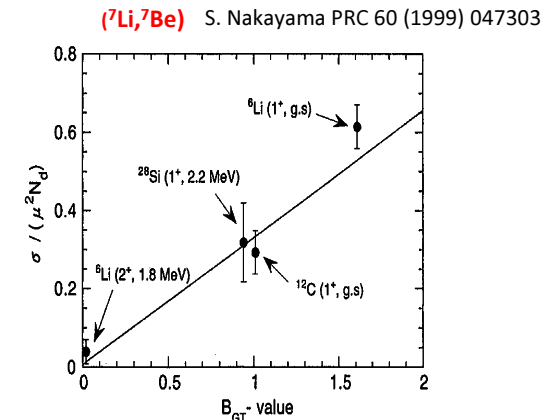


Fig. 18. Cross-sections  $\sigma / (\mu^2 N_d)$  for  $G^+$  transitions in the  $({}^7\text{Li}, {}^7\text{Be})$  reactions at 03 and  $B(G^+)$  values.  $\mu$  and  $N_d$  are the reduced mass and the distortion factor, respectively [197].

## More about NME

$$|M_{\varepsilon}^{\beta\beta 0\nu}|^2 = \left| \langle \Psi_f | \hat{O}_{\varepsilon}^{\beta\beta 0\nu} | \Psi_i \rangle \right|^2$$

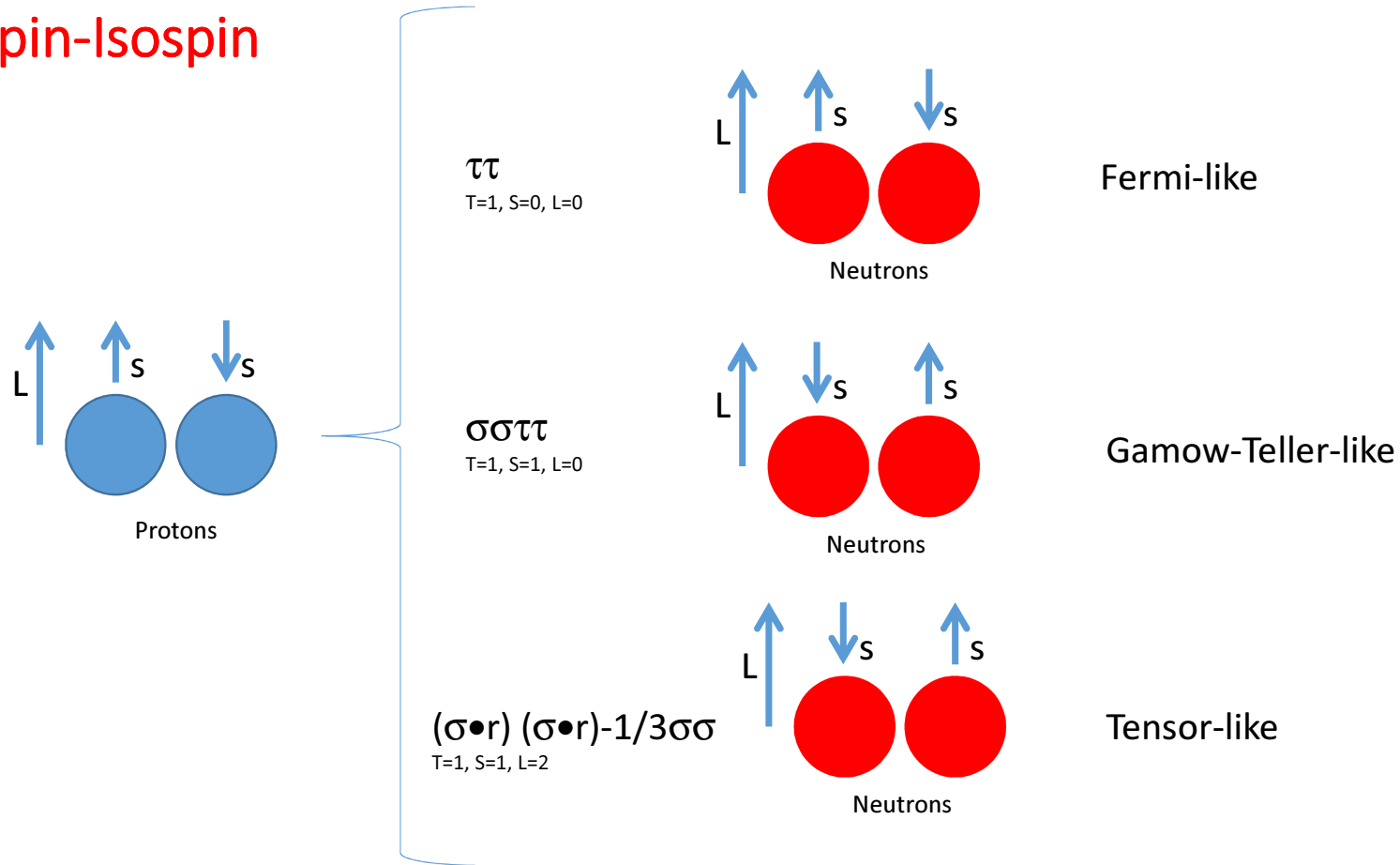
For L = 0 decays

$$\hat{O}_{\varepsilon}^{\beta\beta 0\nu} = \begin{cases} g_A^2 \sum_{i,j} \sigma_i \sigma_j \tau_i \tau_j & \text{Gamow-Teller like} \\ g_V^2 \sum_{i,j} \tau_i \tau_j & \text{Fermi like} \end{cases}$$

Warning: Normally the coupling constants  $g_A$  and  $g_V$  are kept out from the matrix element and we talk of reduced matrix elements

$$|M_{\alpha}^{\beta\beta 0\nu}|^2 = |M_{\alpha}|^2 = B_{\alpha}$$

## Spin-Isospin



The 3 operators are both present in weak and strong interaction

## Radial dependence

$$\Delta r \Delta p \sim h/2\pi$$

$$\Delta r \sim 2 \text{ fm} \quad \longrightarrow \quad \Delta p \sim 0.5 \text{ fm}^{-1} \sim 100 \text{ MeV/c}$$

All the L are possible and as a consequence the operator behaves as the Coulomb potential

$$f(r) \propto 1/r \text{ neutrino potential}$$

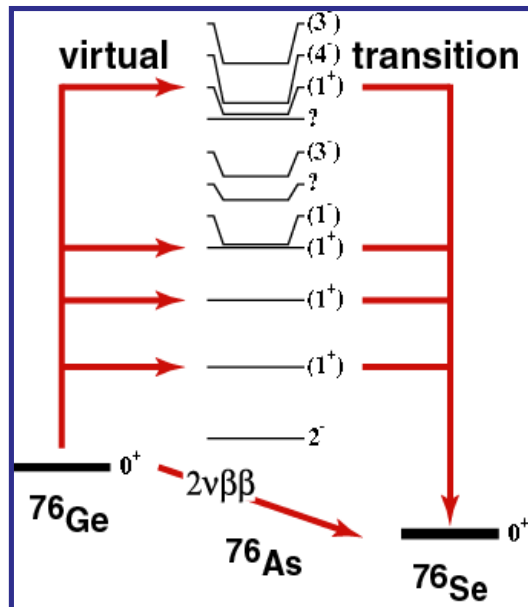
Similarly for the DCE!

# NME: $2\nu\beta\beta$ vs $0\nu\beta\beta$

## NME $2\nu\beta\beta$ - decay

$$1/T_{1/2}^{2\nu}(0^+ \rightarrow 0^+) = G_{2\nu} |M^{\beta\beta 2\nu}|^2$$

q-transfer like ordinary  $\beta$ -decay  
 $(q \sim 0.01 \text{ fm}^{-1} \sim 2 \text{ MeV/c})$   
 only allowed decays possible



Can be determined via charge-exchange reactions in the (n,p) and (p,n) direction ( e.g. (d,<sup>2</sup>He) or (<sup>3</sup>He,t) )

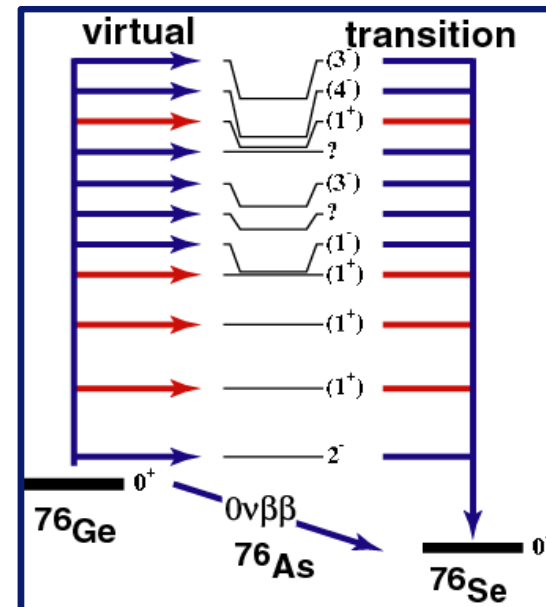
Single state dominance

$$G = \sum_n \frac{|n\rangle\langle n|}{E_n - (E_i + E_f)/2}$$

## NME $0\nu\beta\beta$ - decay

$$1/T_{1/2}^{0\nu}(0^+ \rightarrow 0^+) = G_{0\nu} |M^{\beta\beta 0\nu}|^2 \left| \frac{\langle m_\nu \rangle}{m_e} \right|^2$$

neutrino enters as virtual particle,  
 $q \sim 0.5 \text{ fm}^{-1} (\sim 100 \text{ MeV/c})$   
 degree of forbiddenness weakened



NOT (easily) accessible via charge-exchange reactions

Closure approximation

# The unit cross section

In the  $\sigma(E_p, A)$  the specificity of the single or double charge exchange is express through the **volume integrals of the potentials**: the other factors are general features of the scattering.

## Single charge-exchange

$J_{ST}$  Volume integral of the  $V_{ST}$  potential

## Double charge-exchange

$J_{ST}$  Volume integral of the  $V_{ST}GV_{ST}$  potential, where G is the intermediate channel propagator:

$$G = \sum_n \frac{|\mathbf{n}\rangle\langle\mathbf{n}|}{E_n - (E_i + E_f)/2}$$

where  $E_{i,n,f}$  indicate the energies of the initial, intermediate and final channels, respectively

$E_n$  is a complex number whose imaginary component represents the off-shell propagation through the virtual intermediate states

# The unit cross section

In the  $\sigma(E_p, A)$  the specificity of the single or double charge exchange is express through the **volume integrals of the potentials**: the other factors are general features of the scattering.

## Single charge-exchange

$J_{ST}$  Volume integral of the  $V_{ST}$  potential

## Double charge-exchange

$J_{ST}$  Volume integral of the  $V_{ST}GV_{ST}$  potential, where G is the intermediate channel propagator:

$$G = \sum_n \frac{|n\rangle\langle n|}{E_n - (E_i + E_f)/2}$$

$E_n$  is a complex number whose imaginary component represents the off-shell propagation through the virtual intermediate states

If known  $\sigma(E_p, A)$  would allow to determine the **NME from DCE cross section measurement, whatever is the strength fragmentation**

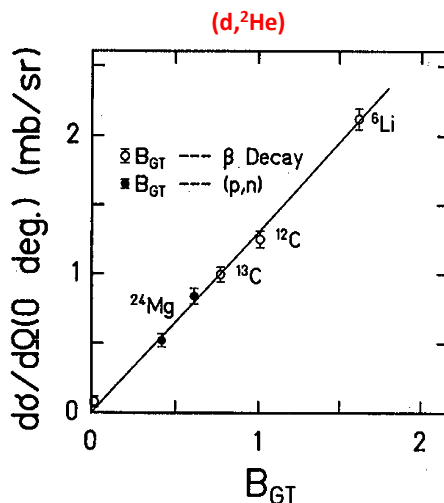


Fig. 12. The measured cross-sections of the  $(d, ^2\text{He})$  reactions at 03 as a function of the  $G^+$  strengths deduced from  $\beta$ -decay or  $(p, n)$  reaction studies. The solid line is a linear "t" to the data [244].

## In single charge exchange reactions

- Y. Fujita Prog. Part. Nucl. Phys. 66 (2011) 549
- F. Osterfeld Rev. Mod. Phys. 64 (1992) 491
- H. Ejiri Phys. Rep. 338 (2000) 256
- T.N. Taddeucci Nucl. Phys. A 469 (1997) 125

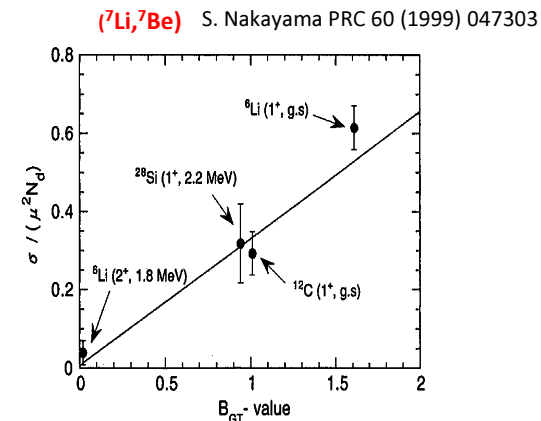


Fig. 18. Cross-sections  $\sigma / (\mu^2 N_d)$  for  $G^+$  transitions in the  $(^7\text{Li}, ^7\text{Be})$  reactions at 03 and  $B(G^+)$  values.  $\mu$  and  $N_d$  are the reduced mass and the distortion factor, respectively [197].

$B(\text{GT}; \text{CEX})/B(\text{GT}; \beta\text{-decay}) \sim 1$  within a few % especially for the strongest transitions

# Search for $0\nu\beta\beta$ decay: a worldwide race

Experiment	Isotope	Lab	Status
GERDA	$^{76}\text{Ge}$	LNGS	Phase I completed Migration to Phase II
CUORE0 /CUORE	$^{130}\text{Te}$	LNGS	Data taking / Construction
Majorana Demonstrator	$^{76}\text{Ge}$	SURF	Construction
SNO+	$^{130}\text{Te}$	SNOLAB	R&D / Construction
SuperNEMO demonstrator	$^{82}\text{Se}$ (or others)		
Candles	$^{48}\text{Ca}$		
COBRA	$^{116}\text{Cd}$	LNGS	R&D
Lucifer	$^{82}\text{Se}$	LNGS	R&D
DCBA	many	[Japan]	R&D
AMoRe	$^{100}\text{Mo}$	[Korea]	R&D
MOON	$^{100}\text{Mo}$	[Japan]	R&D

Neutrino mass explanations: all are based on some form of new physics beyond the Standard Model.  
 Measurement of the neutrino masses and mixing might guide the way toward a Grand Unified Theory of fundamental interactions.

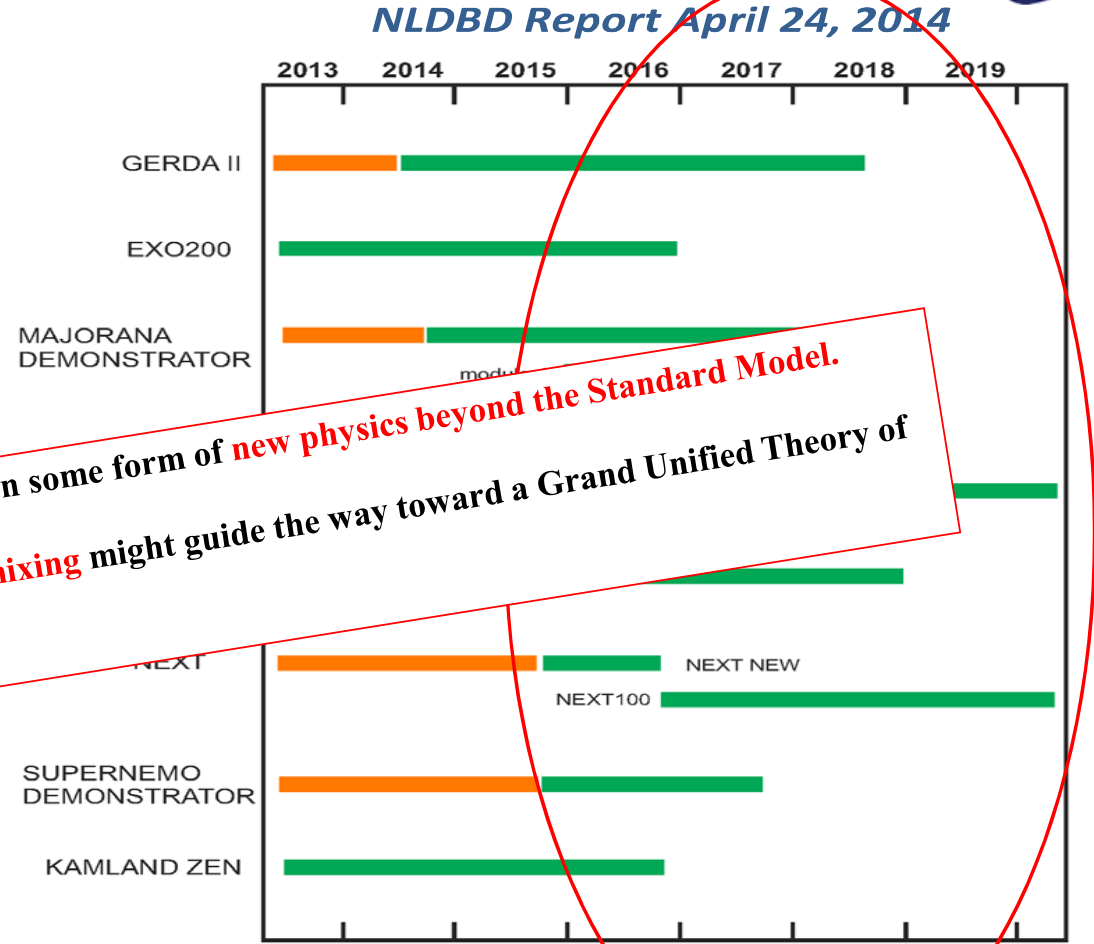
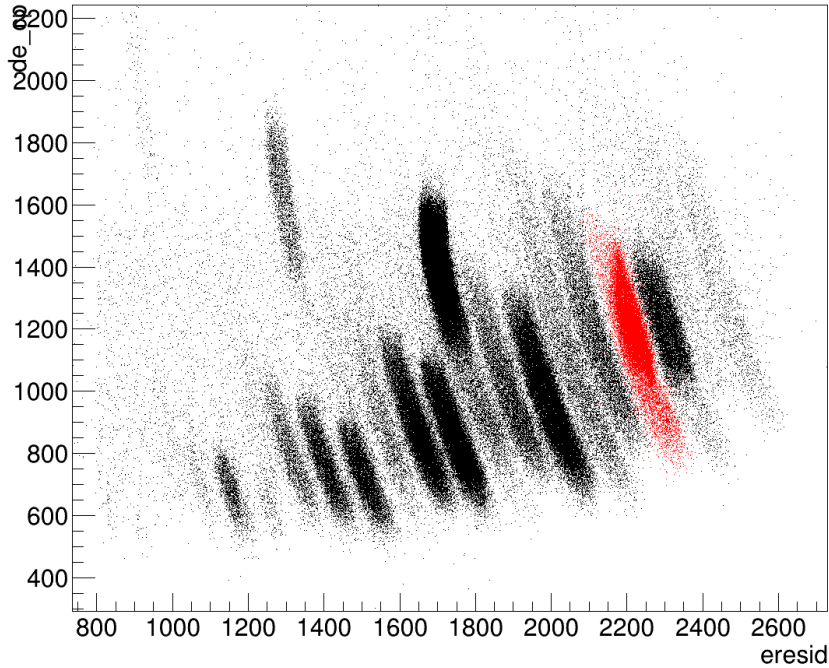
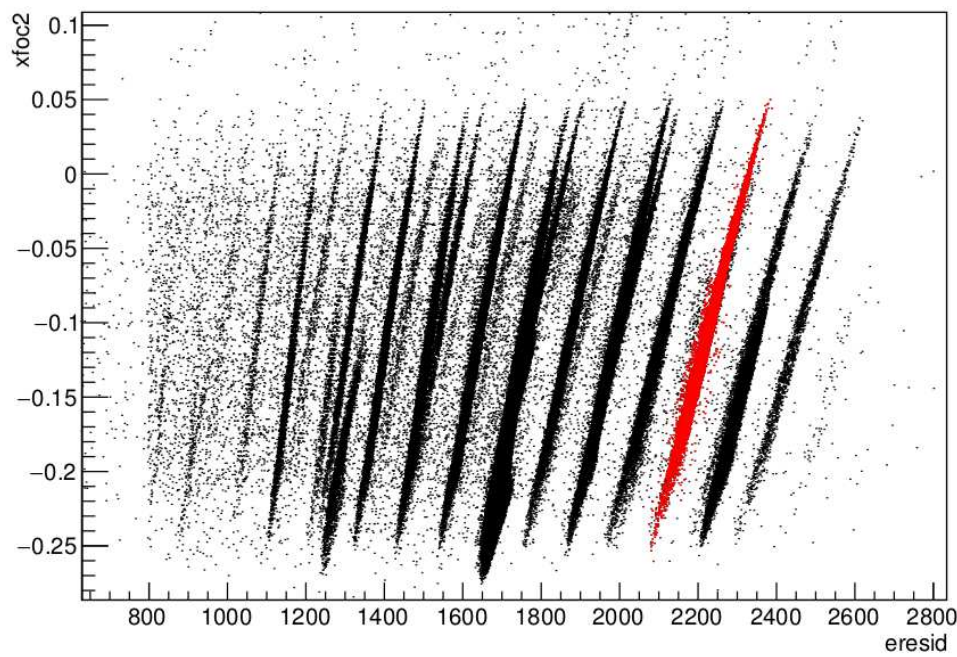


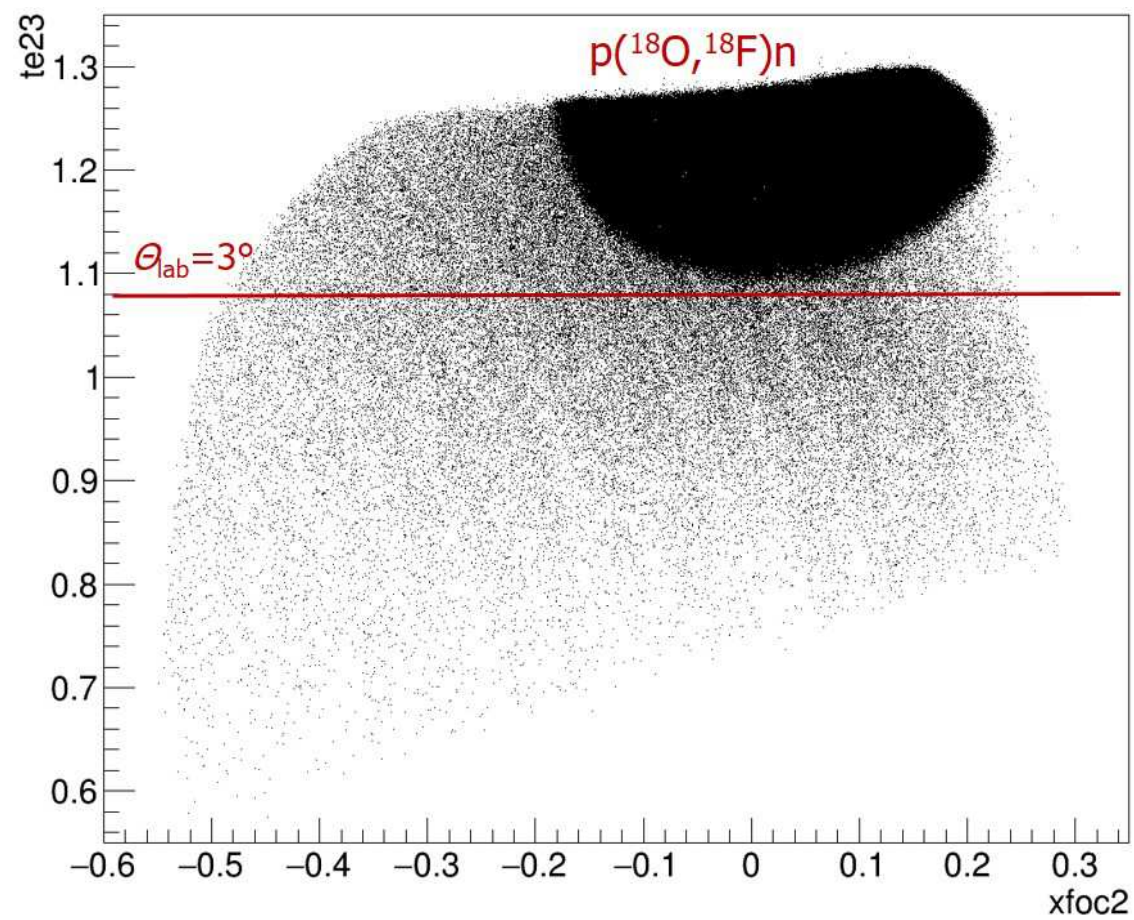
Figure 2.2. Approximate timelines for the presented projects. The orange bars represent nominal construction periods and green illustrates actual or intended running.

# $^{116}\text{Sn}(^{18}\text{O},^{18}\text{F})^{116}\text{In}$ CEX data reduction

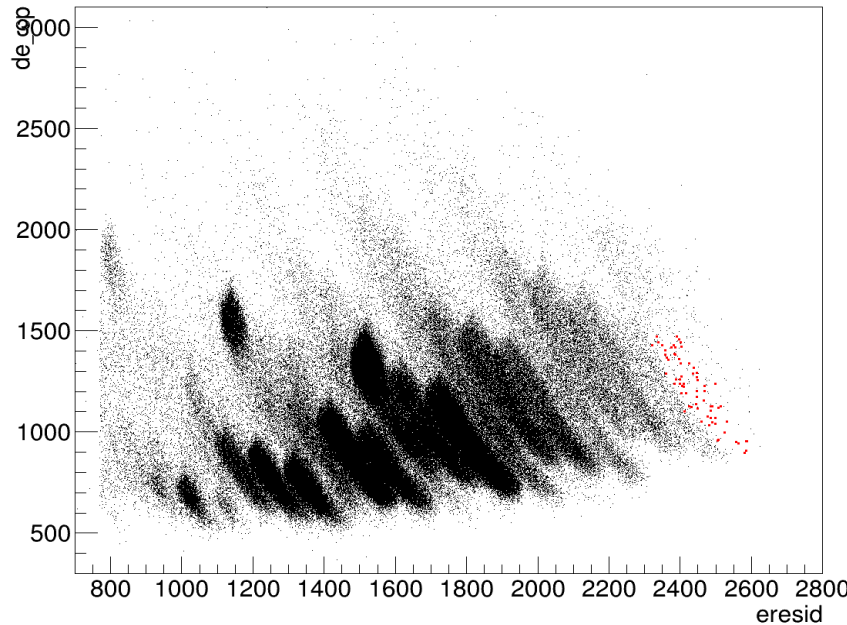


$^{18}\text{F}^{9+}$

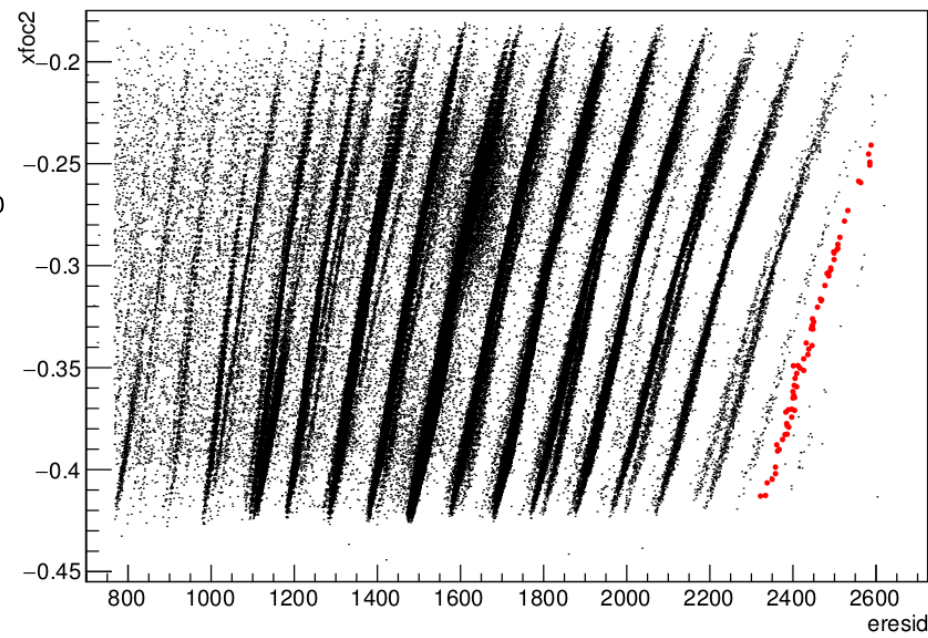




# $^{116}\text{Sn}(^{18}\text{O}, ^{18}\text{Ne})^{116}\text{Cd}$ DCEX data reduction



$^{18}\text{Ne}^{10+}$



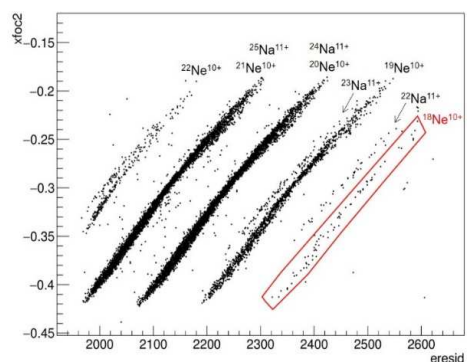
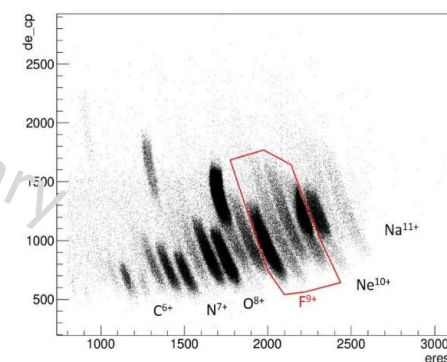
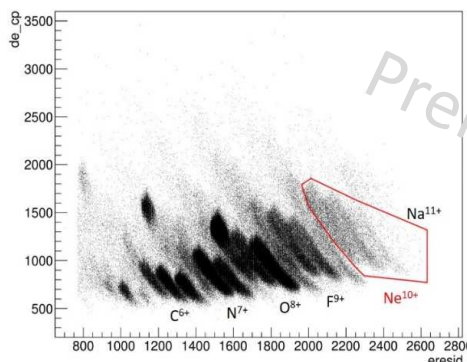


# The experiment

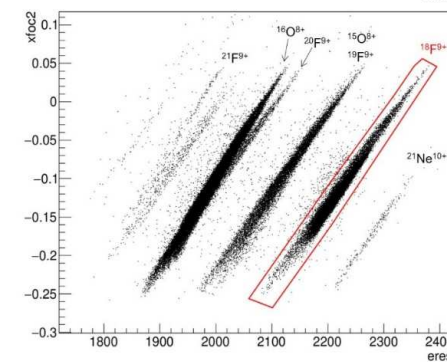
## $^{116}\text{Sn}(\text{O},\text{Ne})^{116}\text{Cd}$ @ 15 MeV/u



- ✓  $E_{\text{beam}} = 15 \text{ MeV/u}$ ,  $^{116}\text{Sn}$  target thickness  $323 \mu\text{g/cm}^2$
- ✓ 2.7 mC integrated charge in 45 BTU
- ✓ Detector and beam transport performances studied up to 8 enA

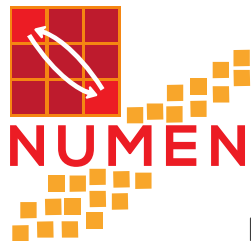


Identification of the Ne Isotopes: <sup>20</sup>Ne(2p channel) and <sup>18</sup>Ne (DCEX)



Identification of <sup>18</sup>F (CEX)

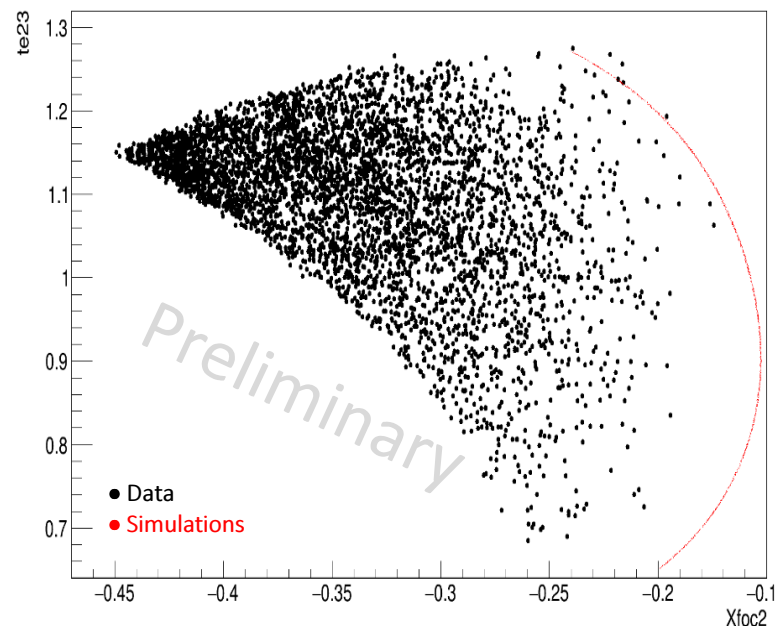




## Study of the $^{18}\text{O} + ^{116}\text{Sn}$ at 15 MeV/u



Partial data-set in the case of identified  $^{18}\text{Ne}$  ejectiles : DCE channel



$\theta_{\text{foc}} - X_{\text{foc}}$  correlation for the identified DCE channel:  $^{116}\text{Sn}(^{18}\text{O}, ^{18}\text{Ne})^{116}\text{Cd}$  at 15 MeV/u.

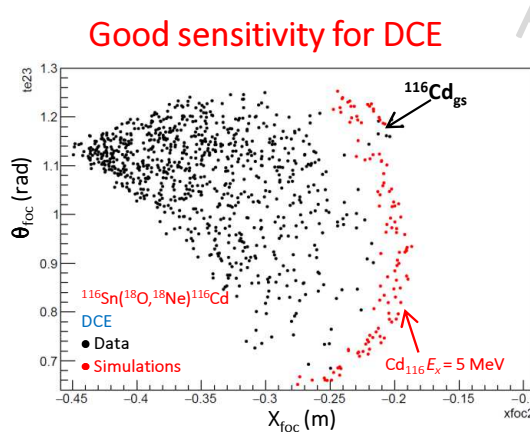
The red line is the result of simulation with a narrow cut in the vertical phase space for the transition to the  $^{116}\text{Cd}_{\text{gs}}$ .



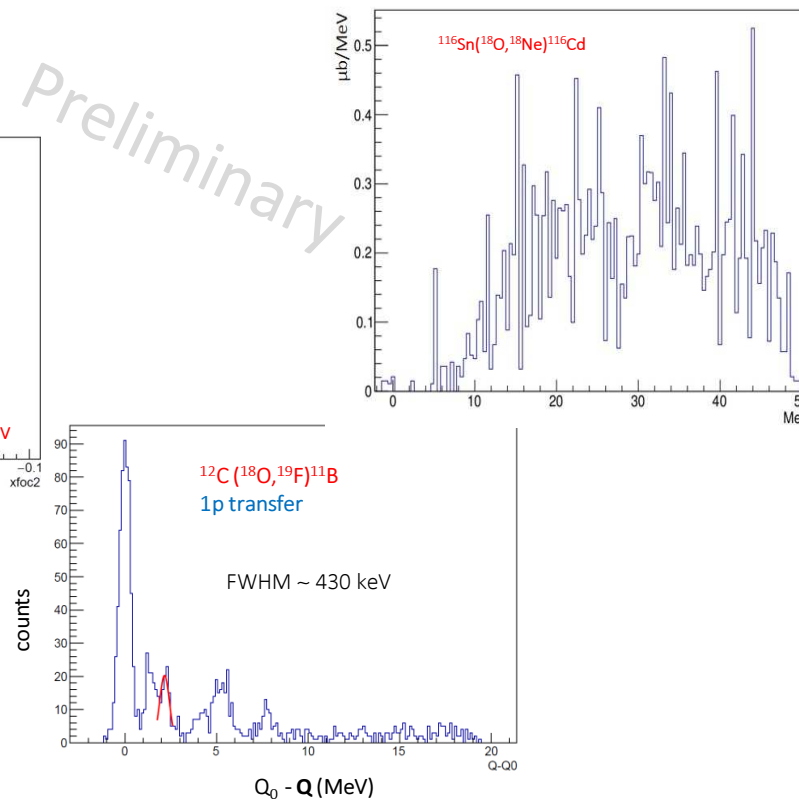
## n on $^{116}\text{Sn}(\text{O}, \text{Ne})^{116}\text{Cd}$

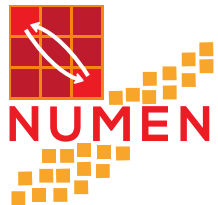


- ✓  $E_{\text{beam}} = 15 \text{ MeV/u}$ , target thickness  $400 \mu\text{g/cm}^2$
- ✓  $150 \mu\text{C}$  integrated charge in 50 hours at 1 enA (including dead time 50%)
- ✓ Detector and beam transport performances studied up to 6 enA
- ✓ Realistic cross section estimate for DCE

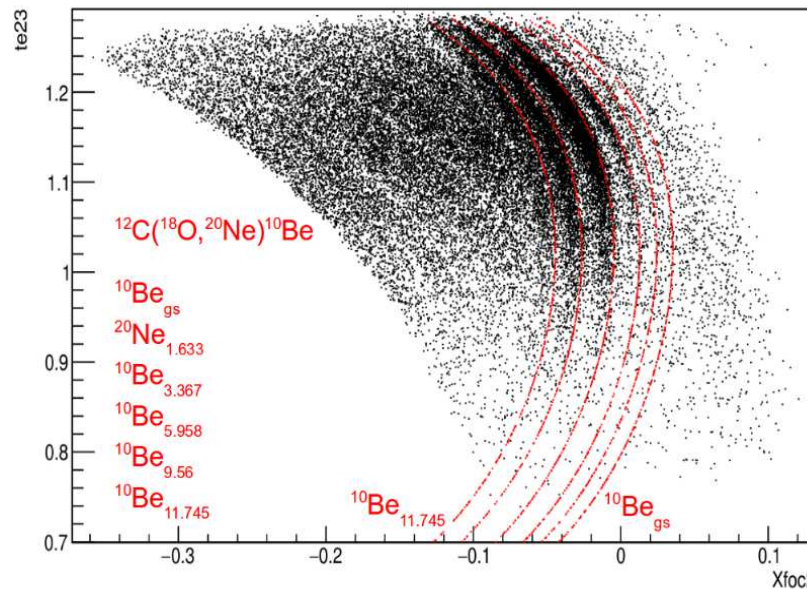
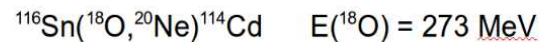


About 4 counts for  
 $^{116}\text{Sn}_{\text{gs}} \rightarrow ^{116}\text{Cd}_{\text{gs}}$



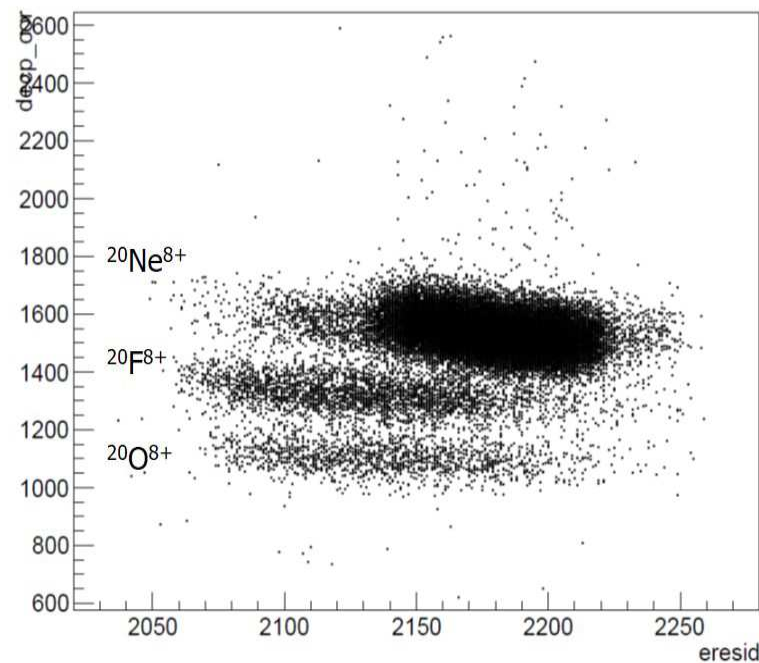
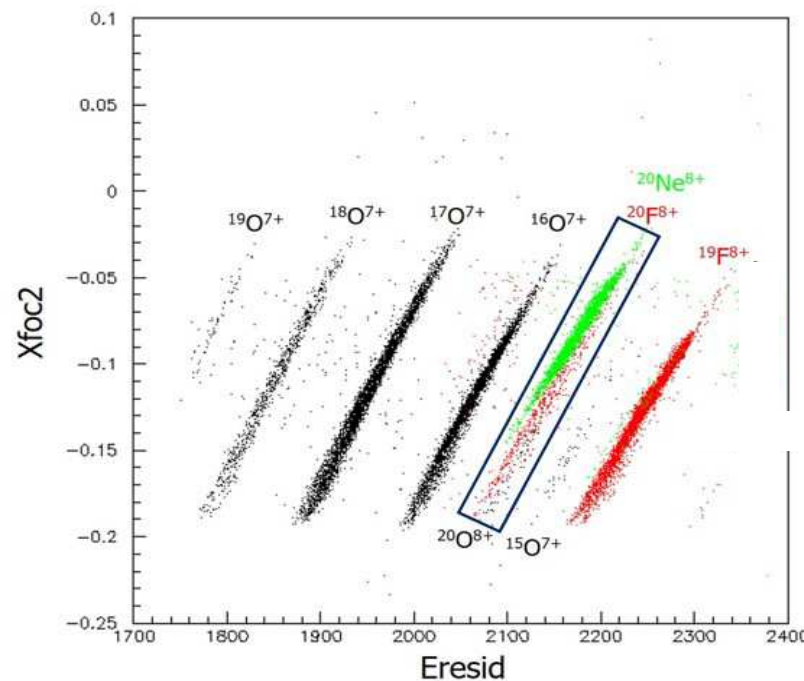


## 12C contaminant in the target

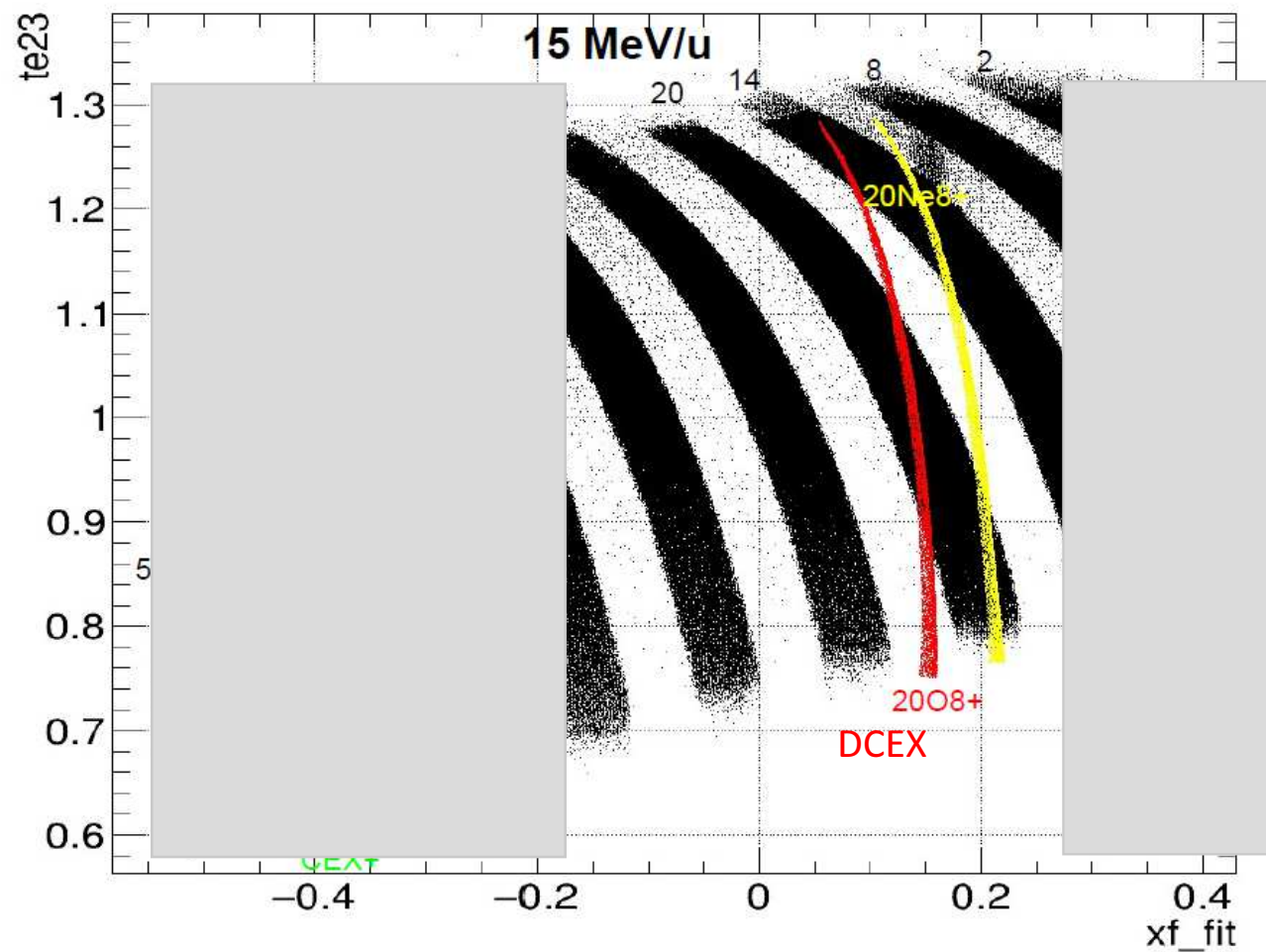


Preliminary plot of the parameters  $\theta_{\text{foc}}$  (horizontal angle) and  $X_{\text{foc}}$  (horizontal position), measured at the focal plane for the selected  $^{20}\text{Ne}$  ejectiles (two-proton transfer channel). The red points in the figure represent the simulated events of the transitions due to  $^{12}\text{C}$  contaminant in the target. The events which are at the right side of the transition to the  $^{12}\text{C}(^{18}\text{O}, ^{20}\text{Ne})^{10}\text{Be}_{\text{g.s.}}$  are due to the  $^{116}\text{Sn}$  and are free from contamination. A supplementary run on carbon target was also performed for background subtraction.

# $^{116}\text{Cd}(\text{Ne}^{20}, \text{O}^{20})^{116}\text{Sn}$ DCEX reaction @ 15 MeV/A



## Experiment at 15 MeV/A





C. Agodi, J. Bellone, R. Bikker, D. Bonanno, D. Bongiovanni, V. Branchina, M.P. Bussa, L. Busso, L. Calabretta, A. Calanna, D. Calvo, F. Cappuzzello, D. Carbone, M. Cavallaro, M. Colonna, G. D'Agostino, N. Deshmukh, S. Ferrero, A. Foti, P. Finocchiaro, G. Giraudo, V. Greco, F. Iazzi, R. Introzzi, G. Lanzalone, A. Lavagno, F. La Via, J.A. Lay, G. Litrico, D. Lo Presti, F. Longhitano, A. Muoio, L. Pandola, F. Pinna, S. Reito, D. Rifuggiato, M.V. Ruslan, G. Santagati, E. Santopinto, L. Scaltrito, S. Tudisco

*INFN - Laboratori Nazionali del Sud, Catania, Italy, INFN - Sezione di Catania, Catania, Italy Dipartimento di Fisica e Astronomia, Università di Catania, Catania, Italy, INFN - Sezione di Torino, Torino, Italy, Politecnico di Torino, Italy INFN - Sezione di Genova, Genova, Italy, CNR-IMM, Sezione di Catania, Italy, Università degli Studi di Enna "Kore", Enna, Italy*

**T. Borello-Lewin, P. N. de Faria, J.L. Ferreira, R. Linares, J. Lubian, N.H. Medina, J.R.B. Oliveira, M.R.D. Rodrigues, D.R. Mendes Junior, V. Zagatto**

*Instituto de Física, Universidade Federal Fluminense, Niterói, RJ, Brazil*

*Instituto de Física, Universidade de São Paulo, São Paulo, SP, Brazil*

**X. Aslanoglou, A. Pakou, O. Sgouros, V. Soukeras, G. Souliotis,**

*Department of Physics and HINP, The University of Ioannina, Ioannina, Greece*

*Department of Chemistry and HINP, National and Kapodistrian University of Athens, Greece*

**E. Aciksoz, I. Boztosun, A. Hacisalihoglu, S.O. Solakci,**

*Akdeniz University, Antalya, Turkey*

**L. Acosta, E.R. Chávez Lomelí,**

*Universidad Nacional Autónoma de México*

**S. Boudhaim, M.L. Bouhssa, Z. Housni, A. Khouaja, J. Inchaou**

*Université Hassan II – Casablanca, Morocco*

**N. Auerbach,**

*School of Physics and Astronomy Tel Aviv University, Israel*

**H. Lenske,**

*University of Giessen, Germany*

**Spokespersons:** C. Agodi ([agodi@lns.infn.it](mailto:agodi@lns.infn.it)), F. Cappuzzello ([cappuzzello@lns.infn.it](mailto:cappuzzello@lns.infn.it)) \